

# UC Irvine

## UC Irvine Electronic Theses and Dissertations

### Title

Breast MRI Segmentation and Density Analysis, 3D Model Reconstruction and Quadrant Regional Segmentation

### Permalink

<https://escholarship.org/uc/item/5p38c1hj>

### Author

Rodriguez Alegre, Irene

### Publication Date

2015

Peer reviewed|Thesis/dissertation

UNIVERSITY OF CALIFORNIA,  
IRVINE

Breast MRI Segmentation and Density Analysis,  
3D Model Reconstruction  
and Quadrant Regional Segmentation

THESIS

Submitted in partial satisfaction of the  
requirements for the degree of

MASTER OF SCIENCE  
in ELECTRICAL ENGINEERING

by

Irene Rodríguez Alegre

Thesis Committee:  
Professor Gultekin Gulsen, Chair  
Professor Min-Ying Lydia Su  
Professor Franco De Flaviis

2015



## TABLE OF CONTENTS

<b>List of Figures</b> .....	<b>iii</b>
<b>List of Tables</b> .....	<b>iv</b>
<b>Acknowledgements</b> .....	<b>v</b>
<b>Abstract of the Thesis</b> .....	<b>vi</b>
<b>Chapter 1 Introduction</b> .....	<b>1</b>
1.1. Breast density and cancer risk prediction .....	1
1.2. The structure of this thesis .....	6
<b>Chapter 2 Breast MRI and Image Segmentation</b> .....	<b>9</b>
2.1. Breast MRI over Mammography .....	9
2.2. Image Segmentation for Breast MRI .....	17
2.3. The template-based segmentation method .....	19
2.4. Application of the segmentation method for a real case .....	22
2.5. Discussion of the results .....	37
<b>Chapter 3 The 3D model representation</b> .....	<b>44</b>
3.1. The objectives of a 3D model reconstruction .....	44
3.2. The 3D breast reconstruction tool .....	47
3.3. A 3D model reconstructed example .....	52
3.4. The 3D video generation .....	56
<b>Chapter 4 The quadrants regional segmentation</b> .....	<b>58</b>
4.1. The interest behind the regional segmentation .....	58
4.2. A regional segmentation study case .....	60
<b>Chapter 5 Summary and conclusions</b> .....	<b>63</b>
<b>References</b> .....	<b>67</b>

## LIST OF FIGURES

Figure 1 - Breast tissues schematic .....	2
Figure 2 - Examples of MRI exams showing different breast density .....	5
Figure 3 - Example of a middle slice in an MRI.....	15
Figure 4 - Menu for the segmentation software .....	23
Figure 5 - Example of the template manual inputs.....	25
Figure 6 - Menu when selecting "Load Breast Image Data".....	28
Figure 7 - Non- fat saturated image .....	29
Figure 8 - Fat saturated image .....	29
Figure 9 - Slice n° 41 with undersegmentation.....	32
Figure 10 - Use of the "Inclusion" tool.....	32
Figure 11 - Use of the "Exclusion" tool.....	33
Figure 12 - Breast L/R cut menu .....	33
Figure 13 - Manually selecting L/R cut.....	33
Figure 14 - Original automatic density segmentation of slice n° 28 .....	35
Figure 15 - Corrected slice n°28 after exclusion .....	35
Figure 16 - Breast Density Histogram .....	37
Figure 17 - Breast before shape correction.....	48
Figure 18 - Breast after direction correction.....	48
Figure 19 - 3D model of the Right Breast.....	52
Figure 20 - 3D model of the Left Breast .....	53
Figure 21 - Left breast 3D model .....	54
Figure 22 - 3D model of the two breasts .....	55
Figure 23 - Video capture showing the two breasts in 3D.....	57
Figure 24 - Left 3D visualization after rotation .....	57
Figure 25 - Left breast inner upper quadrant .....	61
Figure 26 - Left breast outer upper quadrant .....	61
Figure 27 - Left breast inner lower quadrant.....	61
Figure 28 - Left breast outer lower quadrant.....	61
Figure 29 - Right breast outer upper quadrant.....	62
Figure 30 - Right breast inner upper quadrant.....	62
Figure 31 - Right breast outer lower quadrant .....	62
Figure 32 - Right breast inner lower quadrant.....	62

## LIST OF TABLES

Table 1 - Comparison Breast MRI and x-ray mammography.....	16
Table 2 - Comparison of breast tissue results.....	39
Table 3 - Comparison of fibroglandular tissue results.....	41
Table 4 - Comparison of the calculated Density Percentage.....	43

## **ACKNOWLEDGEMENTS**

I would like to express my great appreciation and gratitude to my advisor Professor Min-Ying (Lydia) Su, for being so helpful and for her continuous support during the last few months. Prof. Su offered me valuable advice and suggestions, not only about this thesis but also about my future career.

I am also deeply grateful to Professor Gultekin Gulsen, who also helped me in every stage of this thesis and cared about my improvement. I was lucky to attend and sincerely enjoy both Prof. Gulsen and Prof. Su classes at University of California Irvine where I learned about medical imaging and its applications, and which made me interested in the Center of Functional Onco-Imaging and gave me the opportunity to work on my Master Thesis here.

I would like to sincerely thank Professor Franco de Flaviis. Not only for kindly serving in my thesis committee but also for his support by choosing me as his Teacher Assistant on his classes.

Of course, my deepest gratitude also goes to Prof Roger Rangel and the Balsells Fellowship. It has been a pleasure to be one of the few students chosen for the Balsells Fellowship, and I am honored and grateful for the opportunity to study this Master of Science at University of California, Irvine.

Finally, thank you so much to my family and friends in Spain for their endless love and support.

## **ABSTRACT OF THE THESIS**

Breast MRI Segmentation and Density Analysis, 3D Model Reconstruction  
and Quadrant Regional Segmentation

by

Irene Rodríguez Alegre

Master of Science in Electrical Engineering

University of California, Irvine, 2015

Associate Professor Dr. Gultekin Gulsen, Chair

One of the most helpful factors to consider when evaluating the development of breast cancer is the independent risk factor known as breast density. The breast density factor is the ratio between the volume of fibroglandular tissue to the total volume of the breasts. It is a measurement that always has to be considered by the radiologists for detection and diagnosis of breast cancer.

In this thesis we present an analysis method to calculate this breast density factor, the analysis is based on image segmentation algorithms. The images being segmented come from breast magnetic resonance imaging,



breast MRI, which provides better results than conventional x-ray mammograms.

The first part of this thesis focuses on the breast MRI template-based segmentation method. The implemented method was first proposed by Muqing Lin et al. in our center back in 2010. The developed method is applied to segment the different slices with 1-3 mm thickness obtained for every breast. As also demonstrated in this first part of the thesis, the method provides successful results for segmentation and calculation of the percentage of breast density.

The second part of this thesis is dedicated to describe a method used to reconstruct a 3D model of the breasts from the MRI slices obtained for each patient. The tool performs a breast alignment correction, followed by the 3D reconstruction and a video generation where we can observe the 3D model from different angles and with different rotation and speed.

Finally, the third part of this thesis involves the study of the breasts by the regional segmentation of the quadrants. Several studies have demonstrated that the probability of breast cancer is not the same at every quadrant. Therefore it is an interesting option for the radiologists to be able to observe a 3D representation of the breast divided in quadrants.

# Chapter 1

## Introduction

### 1.1. Breast density and cancer risk prediction

Breast density is a measure used to describe the proportion of the different tissues on a woman's breasts. Breasts are made up of fatty tissue and fibroglandular tissue, which includes the milk ducts and lobules.

Breast density is an important feature about how the breasts look on an x-ray mammogram or on an image from a breast MRI exam. It compares the area of fatty tissue on the breast to the area of fibroglandular tissue. Breast and fibroglandular tissue are denser than fatty tissue and we are interested in calculating this proportion.

High breast density means there is a greater amount of breast and fibroglandular tissue compared to fat, and we study this characteristic because the high breast density has been associated to a higher risk of breast cancer.

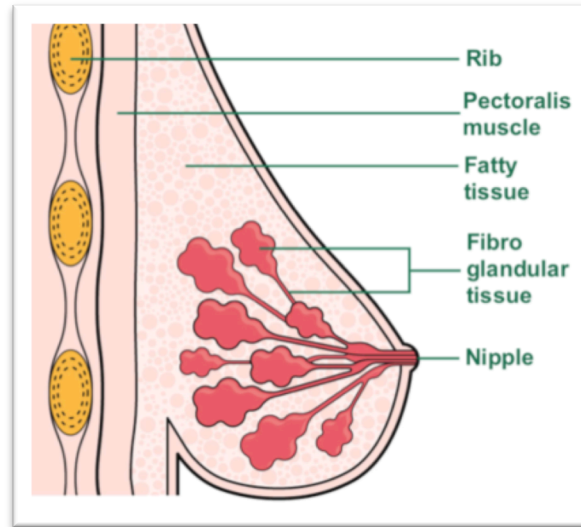


**Figure 1 - Breast tissues schematic**

Figure 1, a modified version of an schematic of the breasts from the MacMillan Cancer Support Organization[1.1], shows the different tissues on a breast.

The most common type of cancer for women around the world is breast cancer, being the second leading cause of cancer death among women. Studies show that over the course of a lifetime, about one every eight women in the U.S. will develop invasive breast cancer. For example in 2013, more than 200,000 new cases of invasive breast cancer were diagnosed in women in the US, along with about 65,000 non-invasive new cases [1.2].

Breast density is an independent risk factor that has been associated [1.3-1.6] with the development of breast cancer.

The fact that dense tissue inside the breasts can obscure lesions is, amongst others, the reason why radiologists always take into consideration breast density factor for a better detection and diagnosis of breast cancer.

The official recognition about the association of higher breast density to an increased risk of breast cancer, has led many organizations to require that women should be informed about their breast density, providing a reliable factor for risk management and a good tool for the evaluation of benefits and risks when considering chemoprevention or hormonal replacement therapy [1.7].

It has been necessary to develop quantitative analysis methods, based on image segmentation algorithms, to be able to measure this breast density factor. In this document we present an image segmentation method that allows the measurement of the breast density factor, the method is template-based. The discussion about the method can be found on Section 2.3.

The density factor between fatty tissue and fibroglandular tissue varies, independently of the size of the breasts and even between the two breasts it can be completely uneven. In Figure 2 we can observe six different cases of non-fat saturated breast MRI middle slices.

Figure 2(a) shows an example where the left breast has really low density, while the right breast is highly dense, and Figure 2(b) represents a case where both breast have similar densities.

Figure 2(a), 2(d) and Figure 2(f) are examples of high breast density, while Figure 2(c) is a case with relatively small breasts but quite dense.

Finally Figure 2(e) on the other hand is a case where the right breast, shown in the left side of the image, received surgery. Therefore we can not assess the density of that breast, and we can only observe low density on the other breast.

It is clear that women with highly dense breasts have more probability of growing cancer, since they have a higher volume of fibroglandular tissue. At the same time, those cases are more complicated to find: malign tissues surrounded by normal tissues and that high density on the breast might make the detection really difficult. In general x-ray mammography presents worse results than breast MRIs, as we will discuss in the next section.

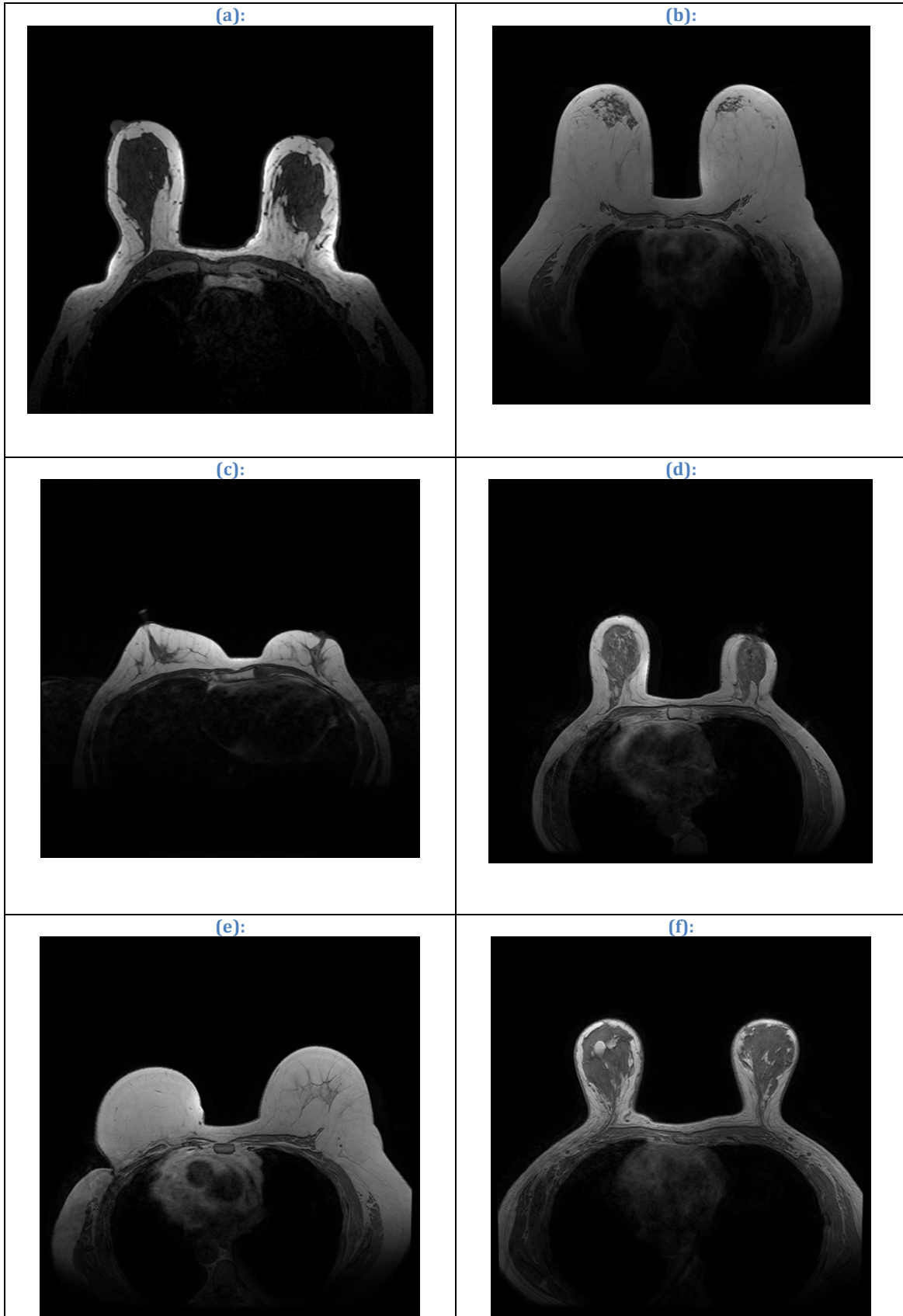


Figure 2 - Examples of MRI exams showing different breast density

## 1.2. The structure of this thesis

In this thesis, we first present an introduction (Chapter 1) including important principles about breast cancer, breast tissues and the breast density risk factor that represents the objective of our data analysis.

To be able to calculate this breast density from the MRI images of the patients we will need to segment those image slices. In Chapter 2 we will discuss the basics about Breast MRI and the Image Segmentation process. Also we will describe the template-based segmentation method used for this thesis, as well as a detailed example of the application of the method. Last, Chapter 2 also includes the discussion of the results of about 270 segmentation cases.

As an aid for radiologists, we determine that having the option to observe the breast MRI data in three-dimensions is actually really helpful for the data visualization. In Chapter 3 we describe a 3D model representation tool that allow us to observe the data in 3D as well as a video generation tool.

In Chapter 4, we study the idea of regional segmentation by dividing the breast in their four quadrants. As described in the chapter, breast cancer risk is different on every quadrant and therefore it is interesting to be able to visualize the data in 3D and divided by quadrants. Chapter 4 includes a discussion about the interest behind the regional segmentation as well as an example study case showing the quadrants representation of a left and right breast MRI exam.

Finally, we can find the summary and conclusions of the thesis in Chapter 5.





## Chapter 2

### Breast MRI and Image Segmentation

#### 2.1. Breast MRI over Mammography

At the Center for Functional Imaging at University of California Irvine, we study magnetic resonance images of the breasts to assess breast density factor on women, as opposed to regular x-ray mammography.

A mammogram is an x-ray picture of the breast that can be used to check for breast cancer in women who have no signs or symptoms of the disease. The process usually involves two x-ray pictures of each breast, which can detect tumors and may also find micro-calcifications (tiny deposits of calcium) that sometimes indicate the presence of breast cancer [2.1].

However, mammograms present certain limitations that are important to be considered.

False-positive results on x-ray mammography occur when radiologists decide mammograms are abnormal but no cancer is actually present. All of these abnormal mammograms should always be followed up with additional testing – involving ultrasound or biopsy – to determine whether cancer is present.

False-positive results are more common for younger women, women who have had previous breast biopsies, women with a family history of breast cancer, and women who are taking estrogen (for example, menopausal hormone therapy). False-positive mammogram results can lead to anxiety and other forms of psychological distress in affected women. The additional testing required to rule out cancer can also be costly and time consuming and can cause physical discomfort.

On the other hand, overdiagnosis and overtreatment might happen when mammograms find cancers and cases of ductal carcinoma in situ that need to be treated. DCIS is a noninvasive tumor in which abnormal cells that may become cancerous build up in the lining of breast ducts.

However, they can also find cancers and cases of DCIS that will never cause symptoms or threaten a woman's life, leading to an overdiagnosis of breast cancer, as well as treatment of these latter cancers and cases of DCIS is not needed and leads to overtreatment. This overtreatment exposes women unnecessarily to the adverse effects associated with cancer therapy. Since doctors often cannot distinguish cancers and cases of DCIS that need to be treated from those that do not, they are all treated.

Radiation exposure is also an important factor on the exams. Mammograms require doses of radiation, and even though the risk of harm from this radiation exposure is extremely low, frequent x-ray exams are not recommended in any case.

Another problem to consider are the False-negative results, which tend to happen too often. False-negatives occur when mammograms appear normal even though breast cancer is present. Overall, screening mammograms miss about 20 percent of breast cancers that are present at the time of screening, which is a large quantity. The main cause of false-negative results is high breast density. False-negative results can lead to delays in treatment and a false sense of security for affected women.

As mentioned previously, breasts contain both dense tissue (i.e., glandular tissue and connective tissue, together known as fibroglandular tissue) and fatty tissue. The most important limitation on x-rays mammograms comes from the fact that fatty tissue appears dark on a mammogram, whereas fibroglandular tissue appears as white areas. Because fibroglandular tissue and tumors have similar density, tumors can be harder to detect in women with denser breasts.

False-negative results occur more often among younger women than among older women because younger women are more likely to have dense breasts. As a woman ages, her breasts usually become more fatty, and false-negative results become less likely.

Finally, results on an x-ray mammogram may also be affected by normal breast overlying lesions that may obscure these lesions and therefore they can not be detected, as well as the negative effect of the calculation of superimposed layers which leads to miscalculations or missing lesions as well as summation artifacts may lead to false results too.

Other features of the mammography exam that may be considered are the discomfort that the patient suffers due to the pressure applied when having the test.

On the other hand, the method that we present is Breast MRI (Magnetic Resonance Imaging) [2.1]. MRI is a procedure in which radio waves and a powerful magnet linked to a computer are used to create detailed pictures of areas inside the body.

These detailed pictures obtained on the exam can show the difference between normal and diseased tissue. Magnetic resonance imaging makes better images of organs and soft tissue than other scanning techniques, such as computed tomography (CT) or x-ray. Magnetic resonance imaging is also highly useful for imaging the brain, the spine, the soft tissue of joints, and the inside of bones.

The breast MRI procedure presents several advantages over the traditional x-ray mammograms.

One of the most important advantages of an MRI exam is that the images are obtained using a big magnet and radio waves. Thus the patient does not receive any ionizing radiation (e.g. x or  $\gamma$  rays).

The exam is performed with the patient laying down, which avoids the high discomfort and pressure of the x-ray mammograms, even though it might feel claustrophobic for some patients.

Another important feature is that MRI provides depth information, which can be analyzed and visualized in 3D. For example we obtain sets of 60 to 180 images per breast. The thickness of the slices varies from 1mm to 3mm.

The image contrast obtained by an MRI exam is really strong, so it is easier to differentiate between fatty tissue and fibroglandular tissue. This feature plus the possibility of a 3D analysis allows a really accurate breast density calculation, which has been determined as an important cancer risk factor that should be considered.

Breast density calculation using MRI can be performed on women with breast implants, and it is specially recommended for cases of high-risk cancer (BRCA1-2, inherited or other genetic disorders).

Unfortunately, the cost of breast MRI exams can be ten times higher than a conventional x-ray mammography.

Figure 3 shows the middle slice of an MRI exam, so we have at our disposition at least 60 more images from that same test. On the other hand, a mammogram would only provide the information obtained by the x-rays in one 2D image (i.e. only 1 image that represents the superposition of all layers of the breast).

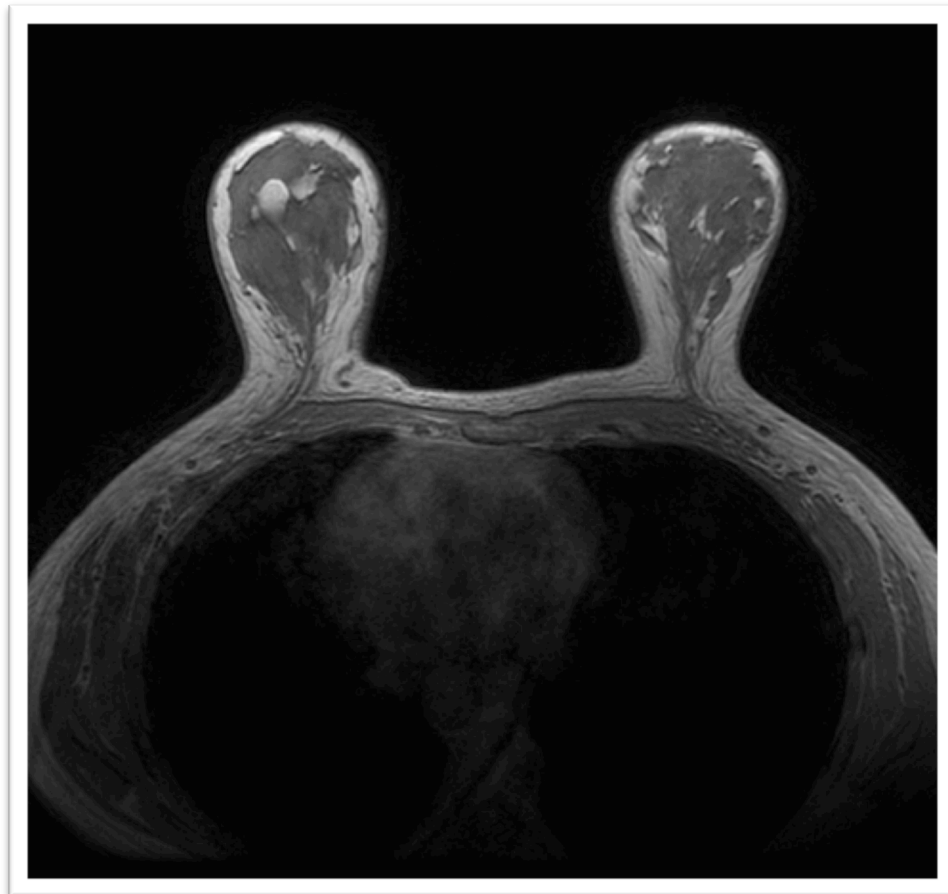


**Figure 3 - Example of a middle slice in an MRI**



We conclude by providing Table 1, a summary of the basic characteristics and differences between an x-ray mammography and a breast MRI exam.

Breast MRI	X-ray mammography
<ul style="list-style-type: none"> <li>✓ No radiation</li> <li>✓ Depth information (+60 slices)</li> <li>✓ 3D analysis and visualization</li> <li>✓ Accurate breast density calculation</li> <li>✓ Strong contrast (fatty tissue vs. fibroglandular tissue)</li> </ul>	<ul style="list-style-type: none"> <li>✗ x-ray radiation</li> <li>✗ Uncomfortable exam (pressure)</li> <li>✗ False results by summation artifacts</li> <li>✗ Lesions might be obscured,</li> <li>✗ Negative superimposition effect</li> <li>✗ Very low image contrast</li> <li>✗ Not good for dense breast</li> </ul>
<ul style="list-style-type: none"> <li>✗ Expensive</li> <li>✗ Might feel claustrophobic</li> </ul>	<ul style="list-style-type: none"> <li>✓ Ten times cheaper than MRI</li> <li>✓ Not-claustrophobic</li> </ul>

**Table 1 - Comparison Breast MRI and x-ray mammography**

## 2.2. Image Segmentation for Breast MRI

In this section we will see the challenges of breast segmentation, describe the segmentation method used designed by Dr. Muqing Lin [2.4] and finally the application of the method for 280 cases, as well as their results.

As discussed in section 2.1, breast MRI is an important tool for breast density analysis [2.6-2.9] and DCE (Dynamic Contrast Enhanced) modality has been used in the screening of high-risk women for the detection and diagnosis of lesions. [2.10-2.13]

Breast MRI obtains 3D images with the particular advantage of providing a strong contrast between fatty tissue and fibroglandular tissue, ideal to calculate the breast density factor.

The first step that has to be performed on the images in order to detect the different tissues, like lesion tissue amongst others, is the image segmentation.

Breast MRI segmentation is a challenging task because breasts can present very different patterns of shape and density, as we saw in Figure 2. But it is a really important task because it provides relevant information that can not be observed visually.

### 2.3. The template-based segmentation method

The segmentation method used on this Thesis was developed in 2012, by Dr. Muqing Lin who was a PhD student at CFOI [2.4]. Before the development of this template-based method, previous studies were performed with other segmentation techniques.

Most research studies used semi-automated methods based on segmentation slice by slice, with the objective of outlining the breast region. This is a task highly time consuming, which requires also individual initializations and corrections.

Lee et al [2.14] used edge detection to determine the breast-air interface and manually outlined the interface between breast and chest wall muscle, on the other hand Khazen et al [2.15] used a thresholding operation to limit the extent of breast volume and manually defined a straight line anterior to the chest wall muscle at each axial slice.

Muqing Lin proposed an innovative automated breast segmentation method that would help develop the computer-aided diagnosis for detection of breast cancer, as well as the quantitative method for analyzing breast density for risk management.

Active contour based methods [2.16-2.17] were applied to detect the boundary of chest wall muscle.

Once completed the segmentation of chest wall muscle, it is still difficult to have robust criteria to define the lateral posterior boundary of bilateral breasts. Nie et al [2.18] used a V-shape cut to exclude the thoracic region and defined the extent of bilateral breasts based on the three anatomical landmarks (the thoracic spine and the lateral margin of the bilateral pectoral muscles). The operator manually selected the landmarks for the V-shape cut and the chest wall muscle was further excluded using B-spline curve fitting.

The methods based on models - instead of using anatomical landmarks for the definition of the extent of bilateral breasts – provide a solution for consistent segmentation as the segmentation for each subject is constrained by the boundary defined by the template.

Gallego et al [2.19] proposed an automated model-based 3D segmentation method which was to first estimate the surface mesh of the subject's breast boundary using edge detection followed by matching the surface meshes between the template and the subject.

In general, most of the model-based segmentation methods create a template that comes from the whole breast volume. But as mentioned earlier, the shape and density pattern of the breasts strongly vary, and therefore using a universal template is not robust enough to segment all types of breast.

However, the region including the heart and the lungs can be detected at similar locations with similar shape and intensity features on the MRI scans. Therefore, a chest body model can be registered to match the subject's specific chest body region, and this deformed chest body model can be further used for segmentation in this subject.

## 2.4. Application of the segmentation method for a real case

In this section, the procedure used for the segmentation study will be described. The example will be based on real cases from exams in 2013.

The segmentation method applied, designed by Muqing Lin [2.4] and mentioned in the previous section, is a template-based breast segmentation method: instead of directly detecting the breast region, the method proposed first generates a template including the chest region contour and also a V-shape landmark, based on the center slice in 2D.

Next, a whole segmentation example will be described.

Once selected a case study, the first step is to analyze how many slices do we have available, since depending on the exam we can have about 60 slices of 3mm thickness, or about 180 of 1mm thickness.

A radiologist determines the first and last slice that has to be segmented, by observing the whole set obtained during the exam. From this subgroup of slices, we select the middle one for initial segmentation.

On the menu for the segmentation software, shown in Figure 4 we first start with “New” on the “Chest Region Template” area. There we will manually select the features on Figure 5, described next.



Figure 4 - Menu for the segmentation software



After loading the center slice, we have to create the template, as shown in Figure 5. To generate the chest region template we need to locate manually the three body landmarks for the V-shape cut on the center slice, as well as the chest region contour. The V-shape landmark is based on three body features: the thoracic spine and the two bilateral boundaries of the pectoral muscle. We identify these three positions to create that V-shape cut that is used to create the subject specific template.

The next step is to manually outline the approximate contour of the chest body region, along the posterior chest wall muscle and outer boundary of the lungs.

From the example in Figure 5, we see how we selected the 3 points of the V-shape (the thoracic spine and the two bilateral boundaries of the breasts) as well as marked the chest region contour. From this information the template will be created, which will be limited by the V-shape, the contour and the air-breast boundary.

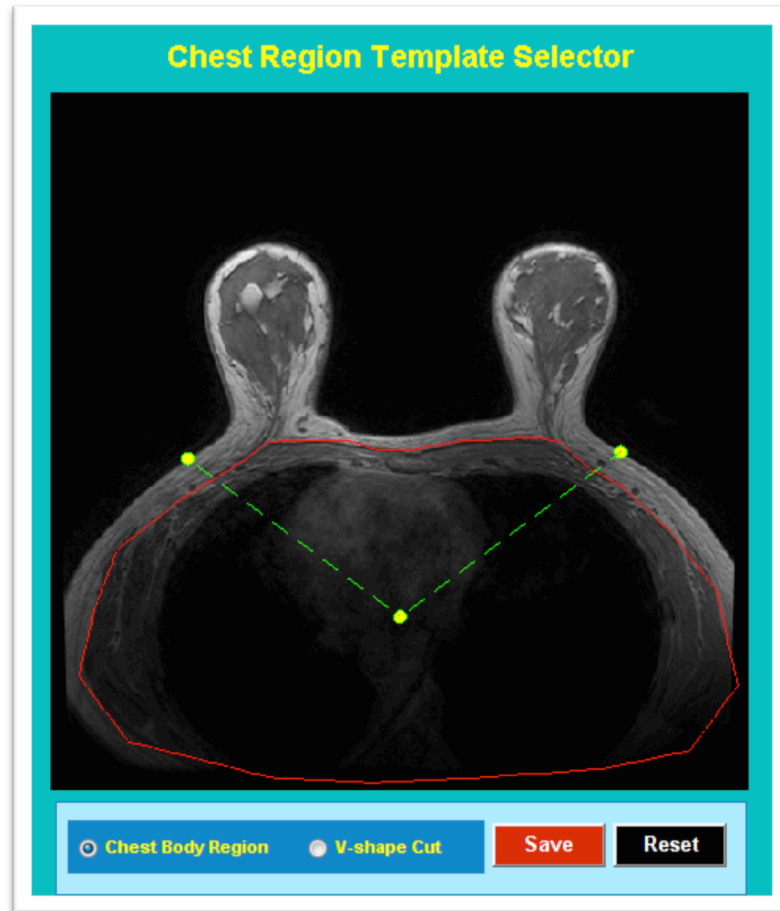


Figure 5 - Example of the template manual inputs

Within this manually drawn region, the k-means clustering algorithm is used to identify dark signal from the lungs and redefine the chest template.

Indeed, after the removal of background noise and registration of the chest models, it is easy to remove most of the chest body region and therefore obtain the template.

Based on the template and the search area of the chest wall muscle (within 15mm from the bottom of the breast boundary) the next step is to detect the chest wall edge, using canny edge detection combined with k-means to improve accuracy.

After the chest region is identified, we exclude it. Then the image is smoothed, normalized and cropped to create the so-called SNC image for registration.

To have the registration process focused on the chest region, the image is cropped 8mm above the chest model contour. The final SNC image of the chest region template is achieved after normalizing with k-means clustering algorithm and smoothed with a Gaussian filter to achieve optimal quality in registration. We work with SNC images to generate subject-specific chest models to use.

The next step is the registration between the chest region template and the subject-specific chest region.

The chest region on the middle slice includes lungs and heart with different signal intensities.

One task is estimating the air region (lung tissue) inside the chest to generate the chest contour that will be coregistered to locate the air (dark region) inside the lungs.

The following step is the exclusion of residual chest wall muscle.

Once the template is ready, on the menu we can go ahead and “Load Breast Image Data” as shown in Figure 6. Also we input the slice range decided by the radiologist, which determines the slice range considered for the study. On the example on Figure 6, we selected the breast range from slices 10 to 53 (out of a total of 64 slices of 3 mm thickness).

Before running the “Start Breast Segmentation” on the software (shown in Figure 6) we need to select if our batch of images is Fat-Sat (fat saturated image) or Non-Fat Sat (non- fat saturated image).

Below we can see examples of the both cases, shown in Figure 7 and Figure 8.

Breast Segmentation

Chest Region Template

Load
New

N3 Correction
  SNC Image

Breast Image Volume

Load Breast Image Data

Slice Range: 10 ~ 32 ~ 53

Voxel Size: 0.703 × 0.703 × 3 mm<sup>3</sup>

Canny Thd : 0.1   0.2

Sigma : 0.5   0.5

Step Length : 1   1

Non-Fat Sat
  Fat Sat

Start Breast Segmentation

Load Existed Breast Segmentation

Check/Modify Breast Segmentation

Left/Right Breast Cut

Show Breast Image Volume

L/R Cut: 0 (Width = 512)

Breast Segmentation Loaded!

Fibroglandular Tissue Segmentation

Density Segmentation Setting

Slice Range: 0 ~ 0

# of Clusters: 2 out of 5

Bias Field Correction

N3    N3+FCM    CLIC

Start Density Segmentation

Load Existed Density Segmentation

Check/Modify Density Segmentation

Fibro Status

Output

.mat File
  Image Sequence
  .txt File
  Color-coded Mask

Save

Breast Segmentation    Density Segmentation

Left Breast    Right Breast    Both Breasts

Breast Volume	Density Volume	Density %
1897 (cc)	0 (cc)	0%
Left Breast	Left Density	Left %
0 (cc)	0 (cc)	0%
Right Breast	Right Density	Right %
0 (cc)	0 (cc)	0%

Results

Figure 6 - Menu when selecting "Load Breast Image Data"



Figure 7 - Non- fat saturated image

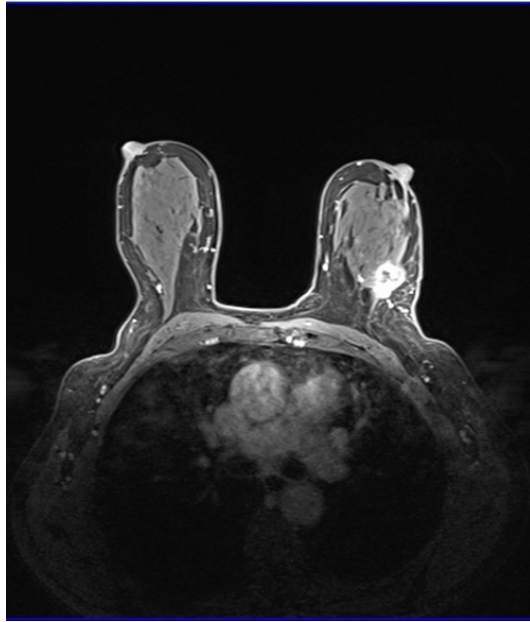


Figure 8 - Fat saturated image

At that point we can go ahead and “Start Breast Segmentation”. The two-dimensional center slice is then segmented by the template. The obtained chest model is used as the template for the next adjacent slice on each side. The template is updated every time and used for the two following slices, and the process continues. Also the previous slice serves as a reference for the identified chest wall boundary. This boundary moves inward 6mm and the segmentation of the chest muscle for the current slice is detected based on the updated chest wall template.

The segmentation of all MRI slices starts on the central slice. After the segmentation of the breast region on that slice has been performed, the chest model for that middle slice is used as a reference for the adjacent ones.

The boundary of those two will be used for the two following, and the process continues superiorly and inferiorly until all slices have been segmented. The idea is based on the fact that there is often high correlation between two adjacent MR slices, since each one is only between 1 mm and 3 mm thick.

The template-based breast segmentation method is proven to be very efficient, but we always find the problem of undersegmentation on the last few slices.

This undersegmentation on the last slices happens because the breasts often present large variation at the ends, their shape and density changes abruptly more than 6mm by slice. Therefore the breast template does not work optimally for each of the 60 or 180 slices per breast.

Once obtained the automatic segmented slices, we will manually correct them to obtain the best results possible. In section 2.5 we can see a comparison between the results, that prove that the automatic results are actually quite precise.

To manually correct each one of the slices we need to access the “Check/Modify Breast Segmentation”, seen in Figure 6.

The following figures show an example of the manual correction of the automatic breast segmentation performed. For example we are correcting the slice number 41, which at the beginning presents undersegmentation, as shown in Figure 9.

Therefore, we use the “Inclusion” tool on this slice, to manually select and include the area that was missed. This step is shown in Figure 10.

Then, Figure 11 shows a further correction, were by choosing the “Exclusion” tool we can exclude some of the areas that were selected but didn’t belong to the breast. In both Figures 10 and 11, Red represents the previous area, while Green marks the updated corrected areas.



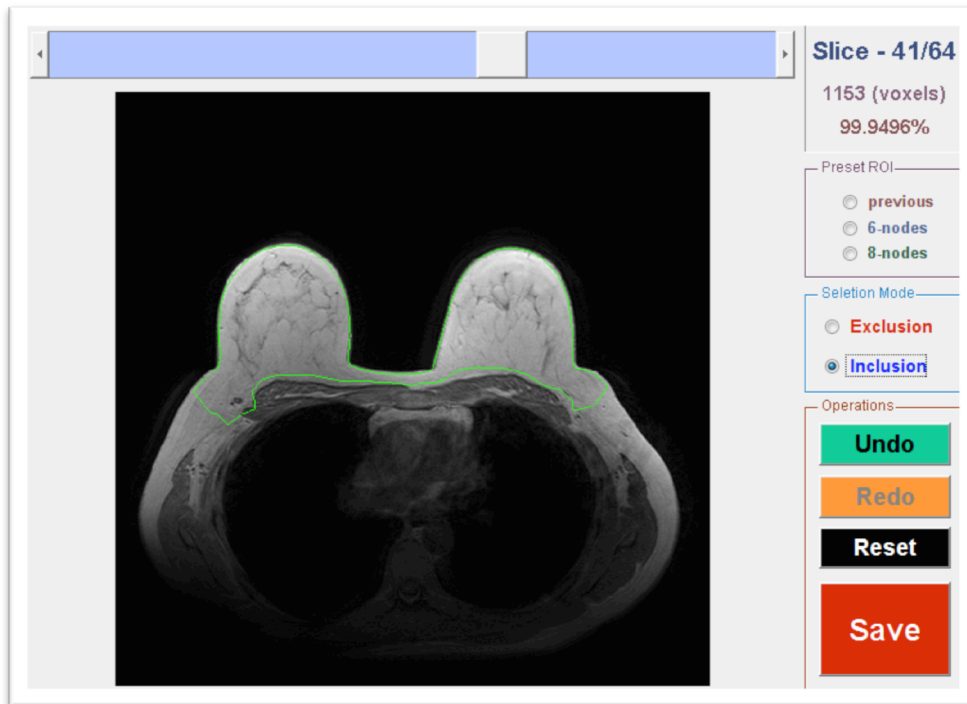


Figure 9 - Slice nº 41 with undersegmentation

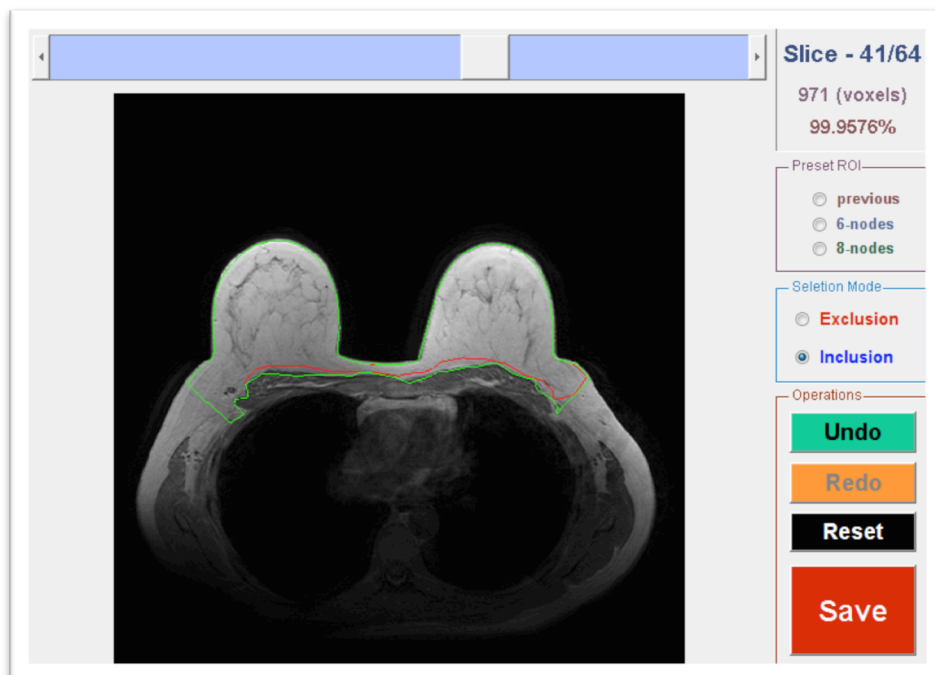


Figure 10 - Use of the "Inclusion" tool

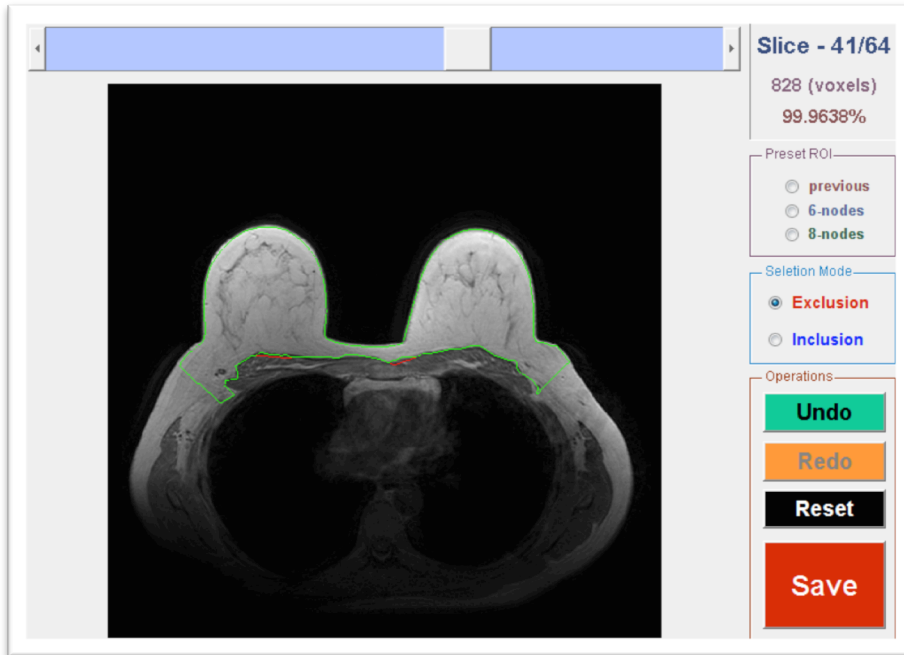


Figure 11 - Use of the "Exclusion" tool

Once we have corrected the breast segmentation on all the slices, we need to select the "Left/Right Breast Cut" on the menu as seen in Figure 12 and Figure 13.

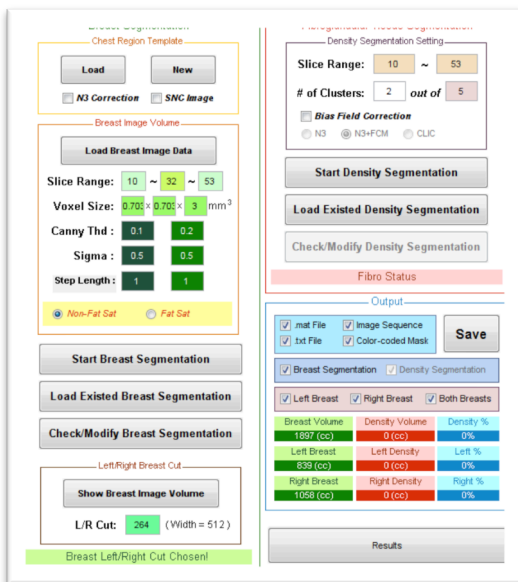


Figure 12 - Breast L/R cut menu

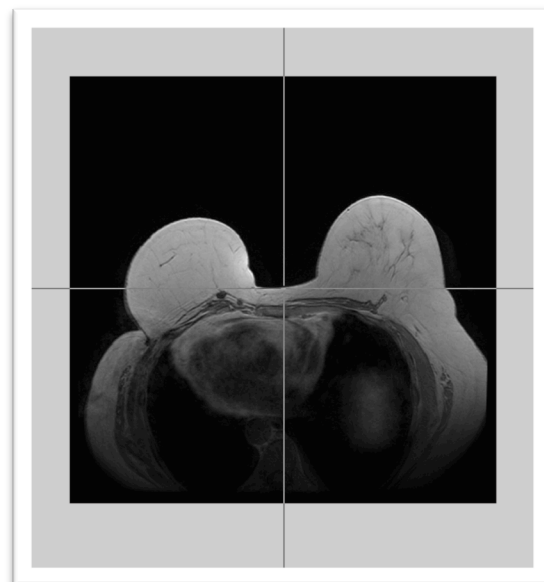


Figure 13 - Manually selecting L/R cut

The next step is to perform the automatic fibroglandular tissue segmentation. To do so we first select, as decided by the radiologist, the slice range where there exists fibroglandular tissue. In this example, as shown in Figure 12, we select the range of slices from 10 to 53.

After the segmentation of the breast region is completed, the next step is to go ahead and “Start Density Segmentation” which will obtain the fibroglandular tissue segmented for that range of slices. The system uses k-means clustering to segment the fibroglandular tissue from the fatty tissue. Bias-field correction algorithm combining N3 and FCM is applied to correct the signal intensity inhomogeneity.

A k-means clustering with  $k=6$  is applied to separate the three lower intensity clusters, which represent the fibroglandular tissue from the three higher intensity ones, which are the fatty tissue. Since there is a really strong image contrast between fat and fibroglandular tissue, the k-means with 6 clusters is good enough for this segmentation.

Similarly to the automatic segmentation of the breast tissue, now we will also need to do some manual corrections, as shown in the following figures.

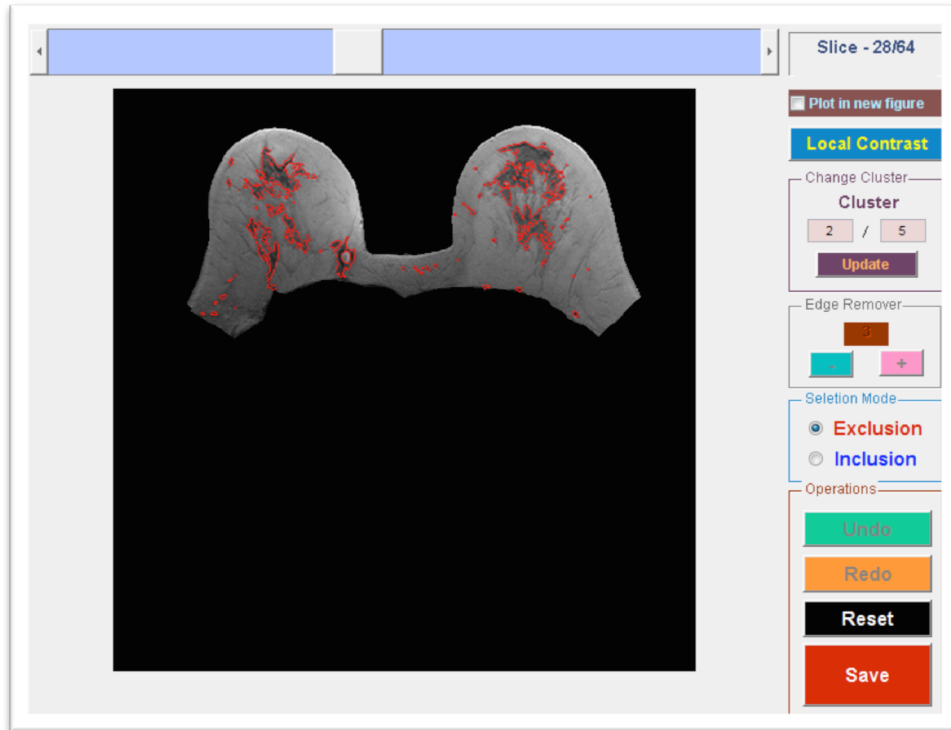


Figure 14 - Original automatic density segmentation of slice n° 28

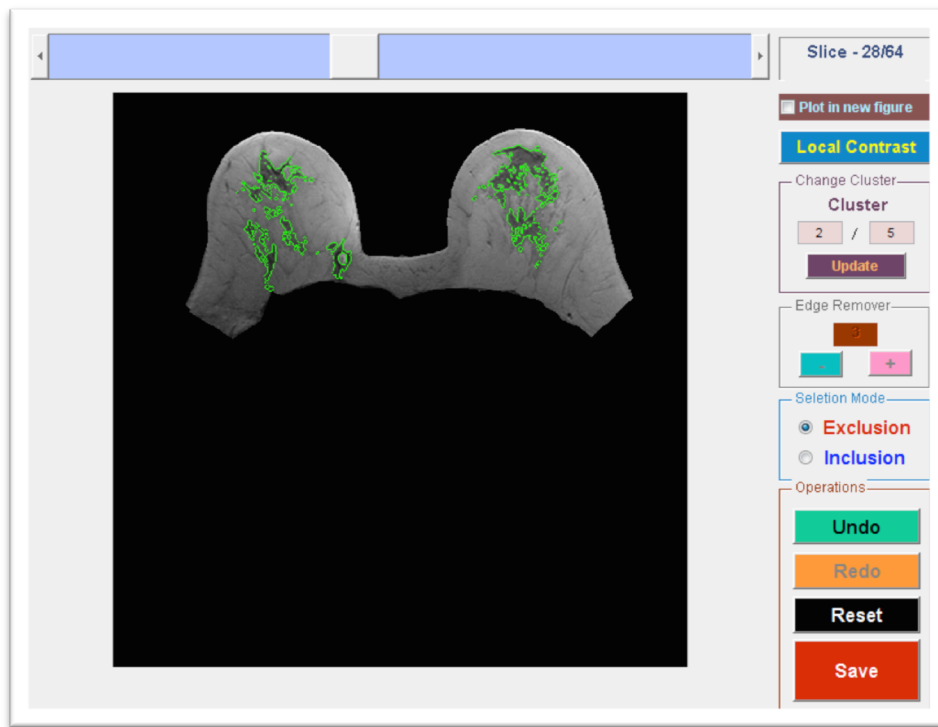


Figure 15 - Corrected slice n°28 after exclusion

In Figure 14 we observe the original fibroglandular segmentation of the 28<sup>th</sup> slice. Some areas have been selected as fibroglandular tissue, but we decide to exclude those points. Refer to Figure 15 for the result of this manual correction.

As shown, the final steps were to evaluate and correct the obtained results. In regards to this, we were offered two manual tools to improve the segmentation: using the inclusion tool we can select breast tissues missed, and using the exclusion tool we can remove tissues that were wrongly included.

Finally, we obtained the desired results. The main purpose of this automated breast segmentation method was for density analysis: the result is the total volume of fibroglandular tissue related to fatty tissue. The automatic segmentation obtained some results, but these are quantitatively compared to the ones of the manually corrected slices. In section 2.5 a comparison of results is presented.

## 2.5. Discussion of the results

In this section we present a variety of results. We will first evaluate the distribution of the calculated breast density factor results. Also we will analyze a series of results about the volume calculations obtained by automatic segmentation of breast tissue and fibroglandular tissue, compared to the volume calculations obtained after manually correcting slice by slice.

After computing the segmentation for 284 breasts, coming from exams taken since 2011, we can provide the following results distribution shown in Figure 16.

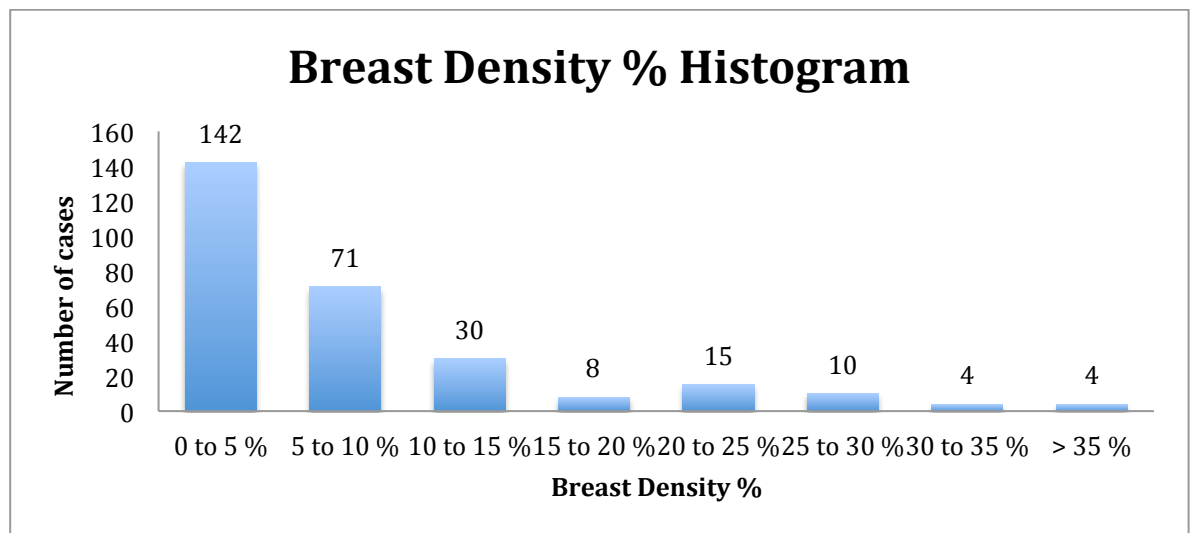


Figure 16 - Breast Density Histogram

It is important to mention that amongst these cases, some of the patients have received some form of surgery, and therefore the density analysis does not represent only healthy breasts.

Next, the analysis of the last fourteen studied cases in 2014 and 2015 is presented. It is interesting to notice that for most of the patients we dispose of two exams taken during two different years. Thus, in total we are comparing “Automatic” and “Manually corrected” volume calculations for 26 situations.

Table 2 (divided in two pages) presents the comparison of Breast volume between the “Automatic” results obtained by the breast segmentation and the “Manually corrected” results after using the manual exclusion and inclusion tools provided on all the slices. By observing the error we can conclude that it is a successful segmentation, even though the manual results are more accurate since we can excel at every slice by manually correcting them all.

Next, Table 3 (divided in two pages as well) presents the comparison of Fibroglandular volume between the “Automatic” results obtained by the breast segmentation and the “Manually corrected” results after using the manual exclusion and inclusion tools.

Table 2 (two pages)

<b>Case ID (year)</b>	<b>Breast L/R</b>	<b>Breast Vol (Manual, cc)</b>	<b>Breast Vol (Auto, cc)</b>	<b>Error %</b>
1095 (2012)	L	1031.7	1023.45	0.8%
	R	1057.4	1069.03	1.1%
1128 (2011)	L	1067.9	1070.04	0.2%
	R	955.74	987.28	3.3%
1128 (2012)	L	1297.92	1325.18	2.1%
	R	1047.14	1072.27	2.4%
1137 (2011)	L	1759.80	1798.52	2.2%
	R	319.92	326.96	2.2%
1137 (2012)	L	1643.67	1681.47	2.3%
	R	403.42	399.79	0.9%
1153 (2012)	L	1134.14	1112.59	1.9%
	R	1212.55	1228.31	1.3%
1153 (2013)	L	1209.233	1235.84	2.2%
	R	1203.98	1241.30	3.1%
1175 (2013)	L	221.23	230.30	4.1%
	R	312.03	321.70	3.1%
1221 (2012)	L	1228.27	1245.47	1.4%
	R	1142.95	1110.95	2.8%
1121 (2013)	L	1036.51	1070.71	3.3%
	R	963.17	974.73	1.2%
1229 (2012)	L	1497.74	1545.67	3.2%
	R	1352.37	1341.55	0.8%
1229 (2013)	L	1442.08	1400.26	2.9%
	R	1403.34	1379.48	1.7%
1234 (2012)	L	485.17	495.84	2.2%
	R	523.58	519.91	0.7%
1234 (2013)	L	431.11	419.47	2.7%
	R	477.42	492.22	3.1%



<b>Case ID (year)</b>	<b>Breast L/R</b>	<b>Breast Vol (Manual, cc)</b>	<b>Breast Vol (Auto., cc)</b>	<b>Error %</b>
1255 (2012)	L	967.78	980.36	1.3%
	R	924.07	898.20	2.8%
1255 (2013)	L	956.86	976.95	2.1%
	R	922.33	904.81	1.9%
1270 (2012)	L	550.80	569.53	3.4%
	R	409.27	401.90	1.8%
1270 (2013)	L	569.12	581.07	2.1%
	R	794.17	820.38	3.3%
1271 (2012)	L	791.11	784.78	0.8%
	R	861.23	862.09	0.1%
1271 (2013)	L	882.80	877.50	0.6%
	R	1073.06	1065.55	0.7%
1332 (2012)	L	343.36	347.82	1.3%
	R	488.25	494.60	1.3%
1332 (2013)	L	364.88	366.34	0.4%
	R	495.25	496.24	0.2%
1372 (2012)	L	757.97	760.24	0.3%
	R	720.19	728.83	1.2%
1372 (2013)	L	802.27	819.12	2.1%
	R	867.78	860.84	0.8%
1376 (2012)	L	1068.63	1061.15	0.7%
	R	828.40	838.34	1.2%
1376 (2013)	L	1072.46	1096.05	2.2%
	R	880.03	900.27	2.3%

Similarly to the Breast Volume results, we see in Table 3 that the error is below the 6% for these cases.

Table 3 (two pages)

Case ID (year)	Breast L/R	Fibroglandular Vol (Manual, cc)	Fibroglandular Vol (Auto, cc)	Error %
1095 (2012)	L	91.58	93.41	2.38%
	R	101.74	104.28	2.88%
1128 (2011)	L	76.70	77.47	1.38%
	R	47.65	49.08	3.38%
1128 (2012)	L	65.59	67.82	3.78%
	R	42.09	42.76	1.98%
1137 (2011)	L	58.43	59.36	1.98%
	R	2.92	2.99	2.88%
1137 (2012)	L	32.22	33.32	3.78%
	R	0.16	0.17	4.78%
1153 (2012)	L	326.11	337.20	3.78%
	R	46.52	47.31	2.08%
1153 (2013)	L	309.95	319.56	3.48%
	R	58.59	60.70	3.98%
1175 (2013)	L	12.17	12.30	1.48%
	R	19.05	19.32	1.78%
1221 (2012)	L	40.49	40.69	0.88%
	R	47.98	49.71	3.98%
1121 (2013)	L	40.00	40.96	2.78%
	R	35.29	36.24	3.08%
1229 (2012)	L	38.18	39.13	2.88%
	R	61.06	62.59	2.88%
1229 (2013)	L	33.82	34.70	2.98%
	R	57.11	57.80	1.58%
1234 (2012)	L	28.05	28.67	2.58%
	R	56.93	57.84	1.98%
1234 (2013)	L	27.08	27.51	1.98%
	R	54.82	55.20	1.08%

<b>Case ID (year)</b>	<b>Breast L/R</b>	<b>Fibroglandular Vol (Manual, cc)</b>	<b>Fibroglandular Vol (Auto, cc)</b>	<b>Error %</b>
1255 (2012)	L	18.49	18.76	1.43%
	R	16.99	17.27	1.64%
1255 (2013)	L	16.69	17.07	2.27%
	R	16.64	17.12	2.89%
1270 (2012)	L	35.60	36.23	1.78%
	R	24.71	25.56	3.43%
1270 (2013)	L	31.26	32.51	3.99%
	R	40.79	41.45	1.63%
1271 (2012)	L	80.00	82.75	3.43%
	R	5.00	5.12	2.40%
1271 (2013)	L	102.04	107.73	5.57%
	R	13.07	13.45	2.87%
1332 (2012)	L	78.02	82.23	5.40%
	R	124.91	130.29	4.31%
1332 (2013)	L	70.41	71.98	2.22%
	R	121.68	124.84	2.59%
1372 (2012)	L	42.39	44.09	4.01%
	R	28.61	29.07	1.60%
1372 (2013)	L	31.77	32.03	0.81%
	R	37.57	38.04	1.26%
1376 (2012)	L	6.93	7.03	1.39%
	R	1.20	1.23	2.23%
1376 (2013)	L	7.19	7.33	1.95%
	R	0.26	0.26	1.08%

Finally Table 4 -in the next page- shows the error for the Density % obtained by the Automatic method and after the manual corrections. Again, we see really successful results.

**Table 4 - Comparison of the calculated Density Percentage**

<b>Case ID (year)</b>	<b>Density % (Manual)</b>	<b>Density % (Automatic)</b>	<b>Percentage Error</b>
1095 (2012)	9.25%	9.48%	2.5%
1128 (2011)	6.08%	6.13%	0.7%
1128 (2012)	4.54%	4.57%	0.7%
1137 (2011)	2.12%	2.12%	0.0%
1137 (2012)	1.00%	1.02%	1.5%
1153 (2012)	16.30%	17.14%	5.2%
1153 (2013)	15.25%	15.43%	1.2%
1175 (2013)	5.80%	5.69%	1.9%
1221 (2012)	3.75%	3.89%	3.7%
1121 (2013)	3.76%	3.79%	0.6%
1229 (2012)	3.53%	3.61%	2.3%
1229 (2013)	3.21%	3.35%	4.3%
1234 (2012)	8.33%	8.48%	1.9%
1234 (2013)	8.88%	8.92%	0.4%
1255 (2012)	1.87%	1.92%	2.3%
1255 (2013)	1.77%	1.82%	2.6%
1270 (2012)	6.25%	6.36%	1.8%
1270 (2013)	5.31%	5.32%	0.2%
1271 (2012)	5.35%	5.57%	4.2%
1271 (2013)	6.39%	6.77%	6.0%
1332 (2012)	24.15%	24.99%	3.5%
1332 (2013)	21.93%	22.40%	2.1%
1372 (2012)	4.78%	4.89%	2.3%
1372 (2013)	4.14%	4.16%	0.5%
1376 (2012)	0.40%	0.40%	1.9%
1376 (2013)	0.35%	0.35%	0.3%

## Chapter 3

### The 3D model representation

#### 3.1. The objectives of a 3D model reconstruction

In this section we will describe a 3D model reconstruction of the breasts, by processing the already segmented data as we discussed in Chapter 2.

We develop a tool to assist radiologists in visually evaluating the change of breast density, by constructing 3D models of the breast and generating a movie.

MRI is an imaging method that obtains a series of images from the patient's body that correspond to slices of only a few mm thickness. We have at our disposition sets of 64 slices of 3 mm thickness, as well as sets of 180 slices of 1 mm thickness.

Not only we can process those images independently, we can also process the whole set later and manage to provide a 3D representation of the breast, making visually easy to evaluate the change of breast density.

It is really helpful to display 3D images of our breast segmentation results, since it makes the understanding and reading of the information much easier. In general, providing three-dimensional models helps in performing tasks like volume calculations, simulations and applications for planning treatments.

However, as mentioned before, not every imaging device can obtain 3D images, most of the times this diagnostic devices are not able to read more than two dimensions and therefore they are unable to even provide data about the third, making impossible to interpret the data and create a 3D model.

On the other hand, by working with MRI radiologists we are able to compare slice by slice the different Breast MRIs of patients taken over time. Therefore, Magnetic Resonance Imaging applied to breast analysis is a very powerful tool in this aspect.

Reviewing the image slices of the patients is indeed very useful, but in some cases it might produce confusion since there could be a small movement of the patient between different exams, which could lead to a misinterpretation of the results shown on the images.

Having to our disposition a 3D version of the information can be really advantageous since the slices are combined, and the radiologists can observe the whole image set.

After working with the segmented images that we obtain, detailed in Chapter 2, we can make a further improvement.

### 3.2. The 3D breast reconstruction tool

We developed a tool to obtain 3D breast models, which is very useful to assist the user or the radiologist's interpretation of the data. The tool provides the possibility of rotating the 3D figure, as well as observe it from different angles and adjust the color and transparency of the fibroglandular tissue and the fatty tissue.

The 3D model is generated on MATLAB, and the complete process is done in three main steps: image segmentation, image correction and creation of the mesh models.

The patient images are obtained on the MRI exam, and segmented using the methods described in Chapter 2. Through this segmentation process we obtain a series of segmented images that include the fibroglandular tissues and the fatty tissues of the different slices, thus the different layers of the breast that have been analyzed by the MRI exam.

Once we have at our disposition the segmented images, an important task is to perform a correction.



Correction is necessary because changing postures of the patient and specific body positions during the MRI exam may lead to a variable image of the breasts, exhibiting visual differences on nipple location and center position respect to the whole breast.

This means that even though we might be observing the breast from the same angle we might see differences that could lead to a false impression. It becomes imperative to perform a correction to create a standard model for every patient case, by correcting the shape and direction of the breasts.

We can see the result of this correction in the next figures. Figure 17 shows the breast as reconstructed from the MRI exam, while Figure 19 represents the corrected breast.

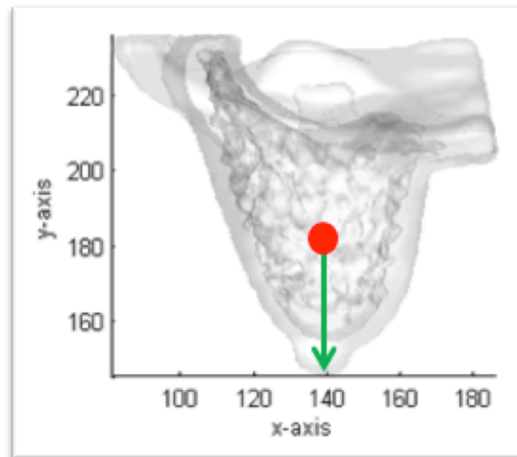
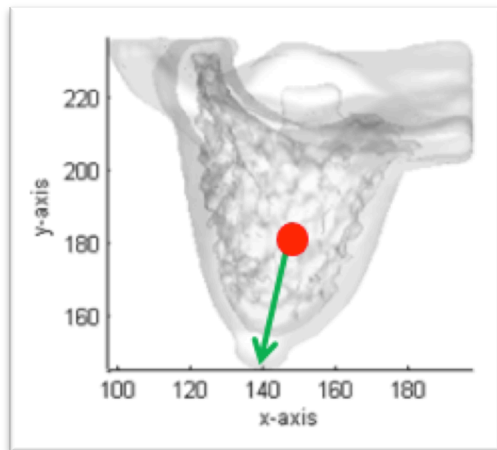


Figure 17 - Breast before shape correction      Figure 18 - Breast after direction correction

For the mentioned correction, we will use the following coordinate system:

- X axis → Horizontal direction (Left/Right)
- Y axis → Vertical direction (Superior/Inferior)
- Z axis → Depth direction (Anterior/Posterior)

By reading the original images, the user has to mark the position of the nipple on the MRI slice, and the following position vector will be obtained.

Nipple position vector:  $[x, y, \text{slice\#}]$

The next step is to combine the breast masks from all the slices, creating a three dimensional matrix of the breast. The original nipple position vector is transformed into the 3D coordinate system and recorded as:

Nipple position at 3D system:  $[x_{nipple}, y_{nipple}, z_{nipple}]$

In addition we need to locate the center of the breast as well, by analyzing the segmented breast mask that we have put together.

We also need to compute the correction offset for each voxel “k” on a z-direction plane:

Center position at 3D system:  $[x_{center}, y_{center}, z_{center}]$

Correction offset:

$$\begin{bmatrix} dx \\ dy \end{bmatrix} = \begin{bmatrix} \frac{x_{nipple} - x_{center}}{z_{nipple} - z_{center}} \cdot (k - z) \\ \frac{y_{nipple} - y_{center}}{z_{nipple} - z_{center}} \cdot (k - z) \end{bmatrix}$$

After the correction offset calculation, each voxel “k” is moved by the offset [dx, dy] along the z-axis.

The same correction procedure is applied to the fibroglandular tissue masks in order to align the data for the fibroglandular data as well.

With the new aligned and corrected updated data we obtain a new 3D matrix of the breasts. And we proceed to the last step: creating a 3D mesh model in Matlab using surface and mesh generation tools, and the new corrected matrix as the input.

Next we process a case from January 2014, that consists of 64 slices of 512x512 pixels.

Every slice is segmented and afterwards it goes through the correction process. The first mask that we obtain is the breast mask, while the second corresponds to the fibroglandular tissue mask.

Therefore we have at our disposition two matrices of size 512x512x64. We have to process these matrices into a 3D breast model.

We include the mesh corresponding to the fibroglandular tissue mask in top of the one corresponding to the breasts, selecting different colors so we can discern them easily, and we align both in the same 3D coordinate system so they correspond. We will not be able to see the fibroglandular tissue, which is inside the breast, unless we set the feature of transparency to the breast tissue.

### 3.3. A 3D model reconstructed example

The 3D models obtained from the 2014-case number 1255 can be observed next. Figure 19 represents the 3D model of the right breast, while Figure 20 is the 3D model of the left breast.

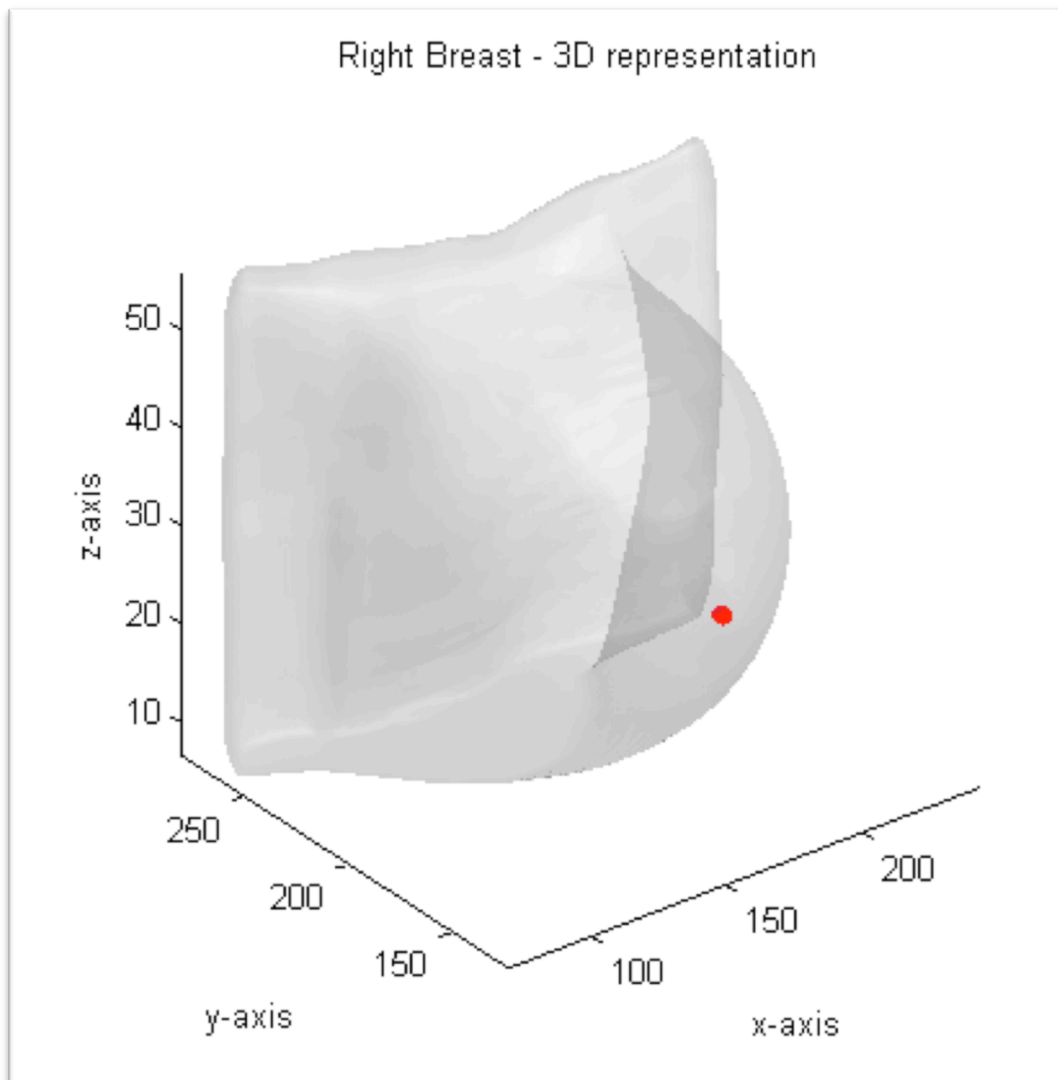


**Figure 19 - 3D model of the Right Breast**

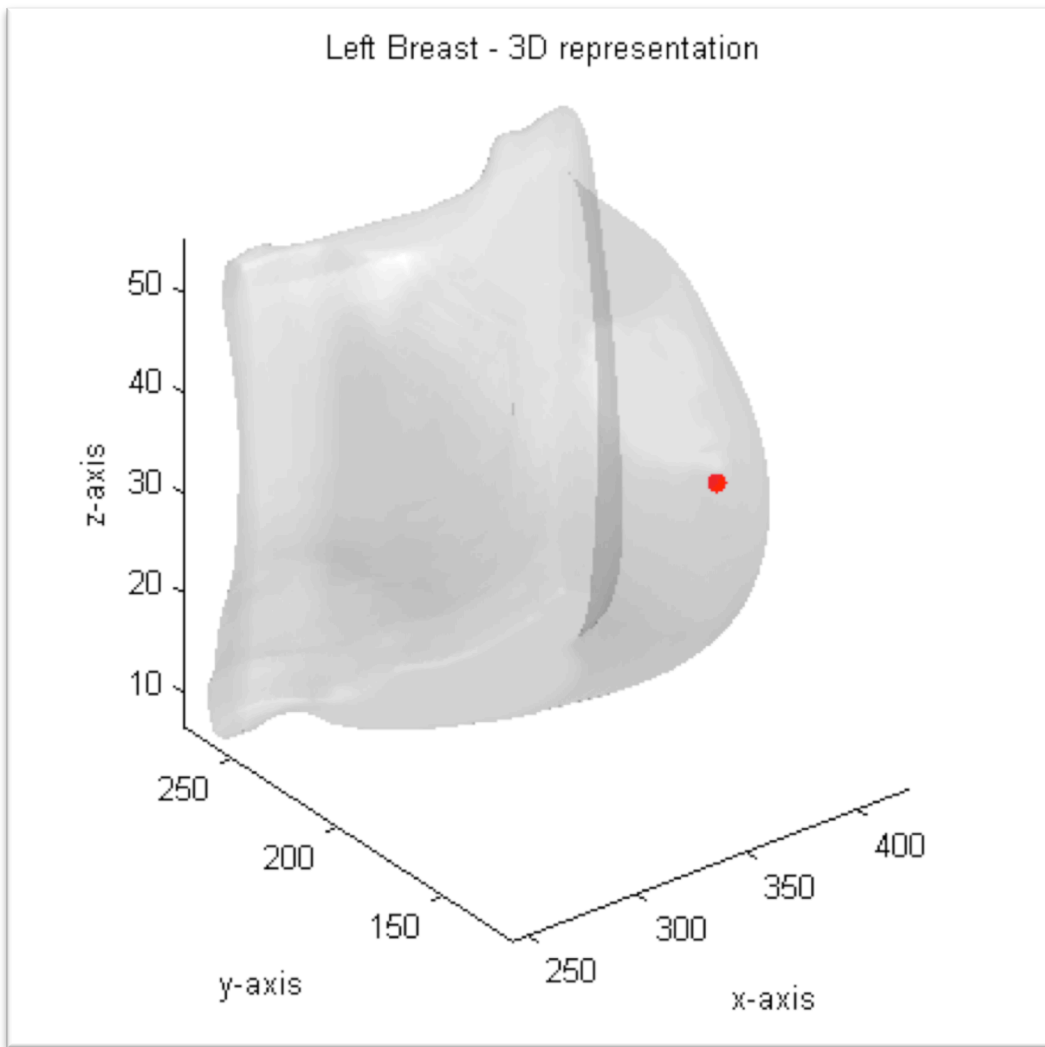


Figure 20 - 3D model of the Left Breast

Figure 21 represents another case, number 1271, where the left breast presents a higher breast density. In this case we can see clearly the fibroglandular tissues.

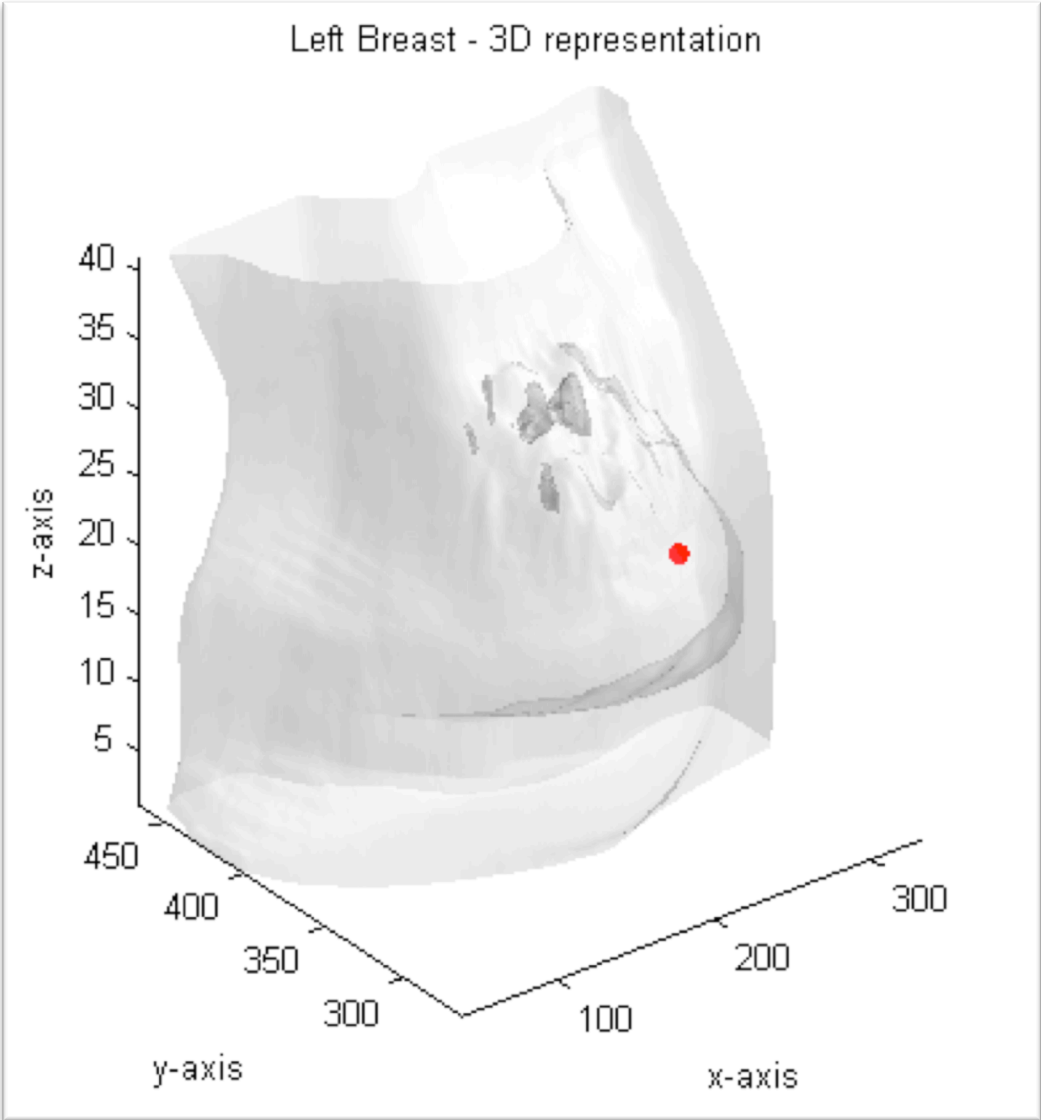
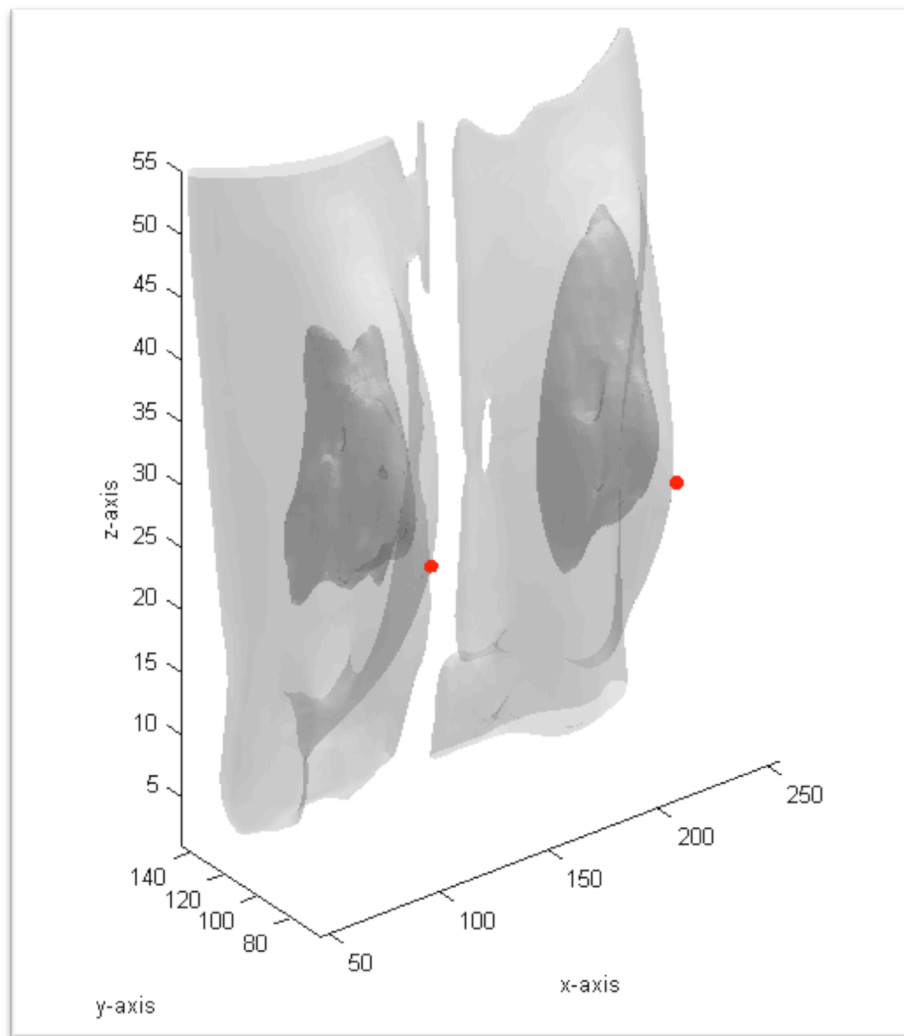


Figure 21 - Left breast 3D model

Finally, case 1332 is shown in Figure 22, where both breast present a high density percentage.

We can see with the two breasts 3D model, how the x-axis represents the frontal direction from right to left. On the y-axis we see the depth, from anterior to posterior, while the z-axis is the up-down direction.



**Figure 22 - 3D model of the two breasts**



### 3.4. The 3D video generation

Not only we can observe in the computer a 3D reconstructed model, we can also generate a video. This video in 3D will automatically rotate and be seen from the angle and rotation speed that we select.

The selection of this settings can be focused on the specific needs that a radiologist might have in different situations, as seen next.

As we can see in Figure 23, one feature on the video is to be able to see the two breasts 3D model.

Under certain circumstances, we might be interested in a single breast view, like the one shown in Figure 24. By using the rotation, we are able to distinguish the small portions of fibroglandular tissue on the outer posterior region of the left breast.

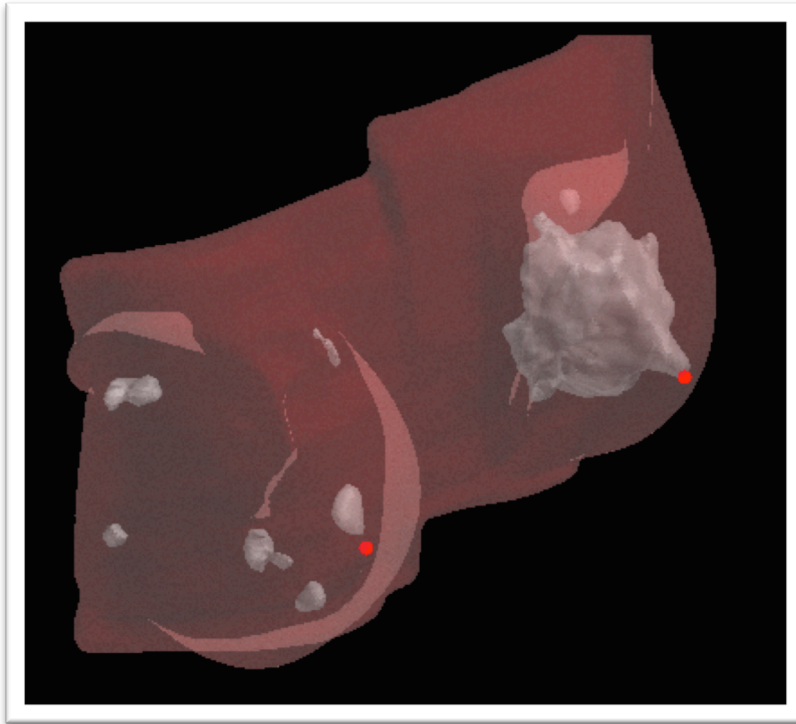


Figure 23 - Video capture showing the two breasts in 3D

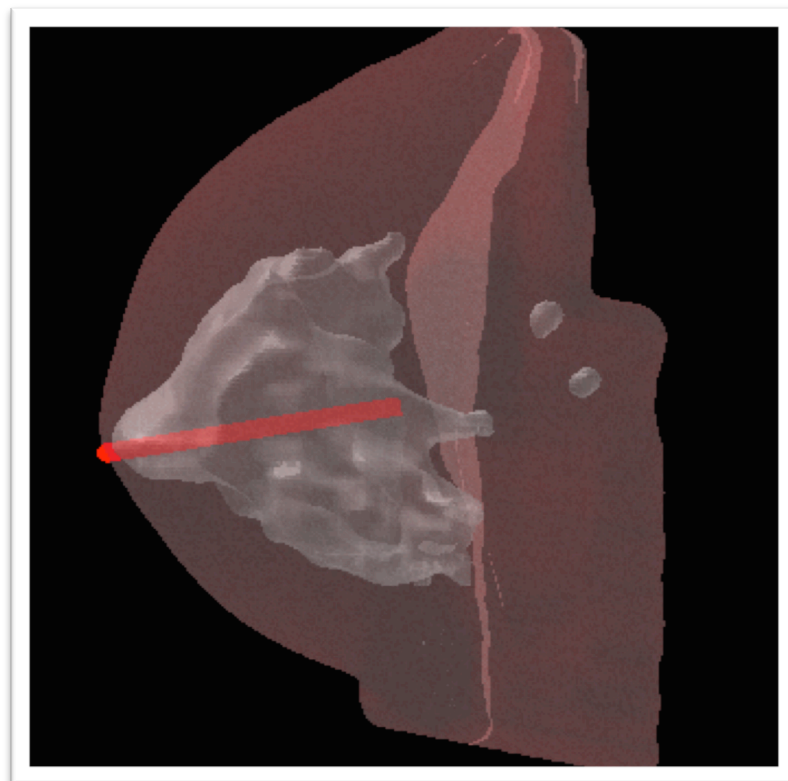


Figure 24 - Left 3D visualization after rotation

## Chapter 4

### The quadrants regional segmentation

#### 4.1. The interest behind the regional segmentation

Several studies have demonstrated that – even in early stage when there is no metastasis or nodal involvement at diagnosis – women with breast cancer localized in the upper outer quadrant have more than double the risk of death than women who have cancer somewhere else in the breast. [4.1-4.3]

The upper outer quadrant was determined to represent 50% of probability of cancer, while the are of the nipple has an approximate 18%, the upper inner quadrant 15% and the lower outer and lower inner 11% and 6% respectively.

These results are proved by a study of 1411 women with Stage 1 breast cancer from 1986 to 2002, from the Swiss registry of breast cancer patients.

Over the 16 years period the study compared mortality risk according to tumor location, adjusted for several risk factors such as age, size and chemotherapy status.

On the other hand, usually the fibrotic changes found in the lower inner quadrant of the breast are more characteristic of benign disorders.

Therefore, since not all breast regions have the same risk of developing a malign case the study of the images by regions of the breast is beneficial to the radiologists because not all regions of the breasts have the same risk of developing cancer. [4.4-4.7]

## 4.2. A regional segmentation study case

Finally, in this section we present an example of a regional segmentation case. We work with the images obtained in 2013 for the case 1332, which we studied in Chapter 3 as well, and we observed their 3D reconstruction together in Figure 22.

After following the procedure and correcting the breast, as described in Chapter 3, section 3.2., we divide the breast into 4 quadrants, being the nipple the center reference.

As seen in Figure 25, the more interesting quadrant might be the upper outer part, since it presents a higher cancer risk.

The results from the 3D representation of the four quadrants segmented are presented next.

Left breast quadrants are shown in Figures 25 to 28, while on the other hand the right breast quadrants are included in Figures 29 to 32.

Notice how we can easily compare which of the quadrants in this case present higher or lower density by observing the 3D representation that includes breast tissue (lighter) and fibroglandular tissue (darker).

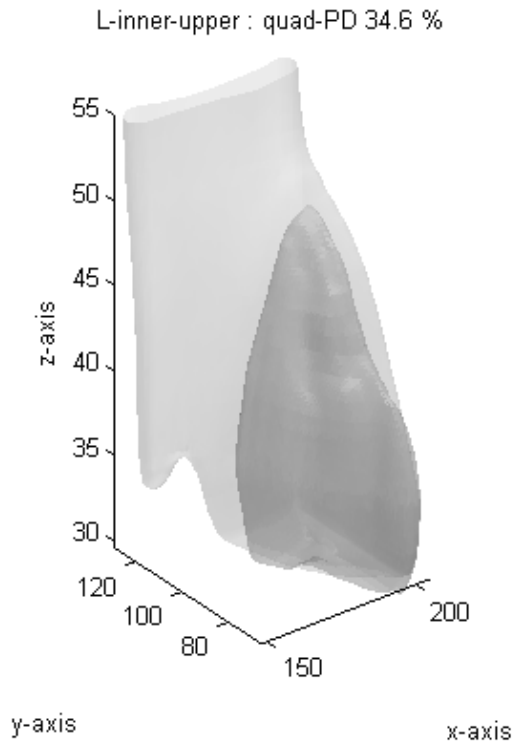


**Figure 25** Left breast inner upper quadrant

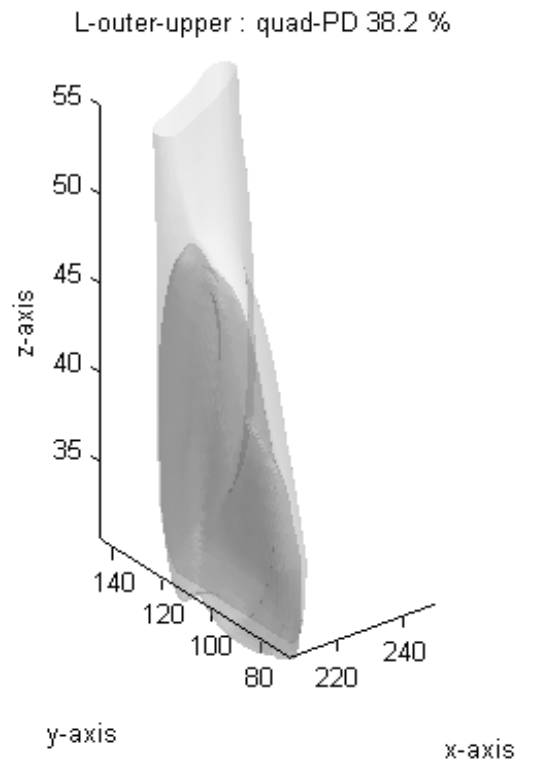


**Figure 26** Left breast outer upper quadrant

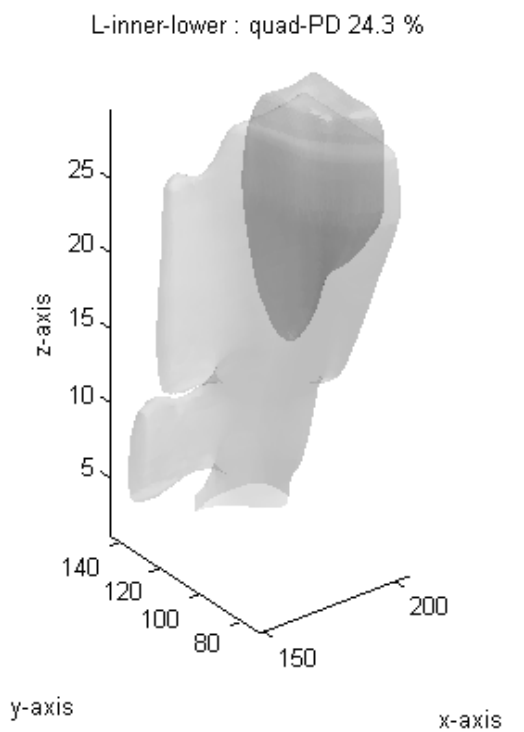


**Figure 27** Left breast inner lower quadrant

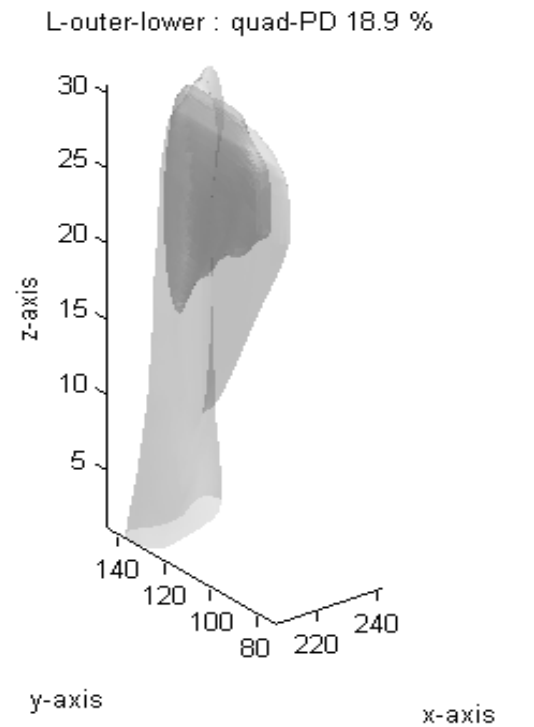


**Figure 28** Left breast outer lower quadrant

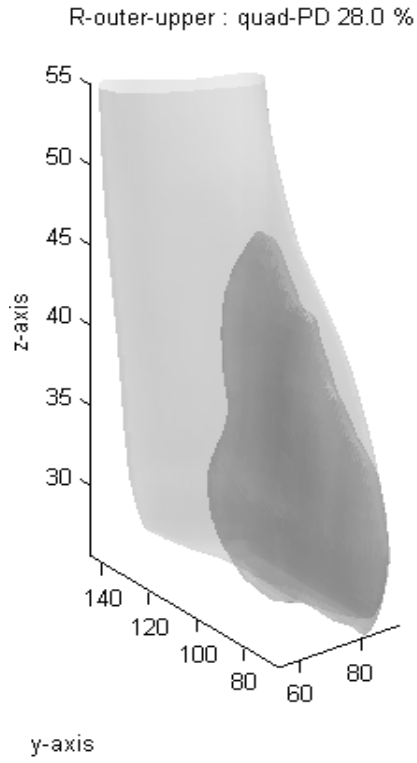


**Figure 29 Right breast outer upper quadrant**

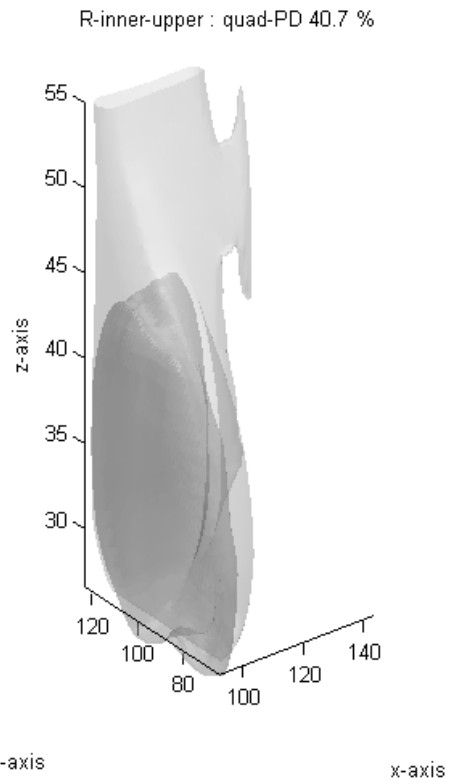


**Figure 30 Right breast inner upper quadrant**

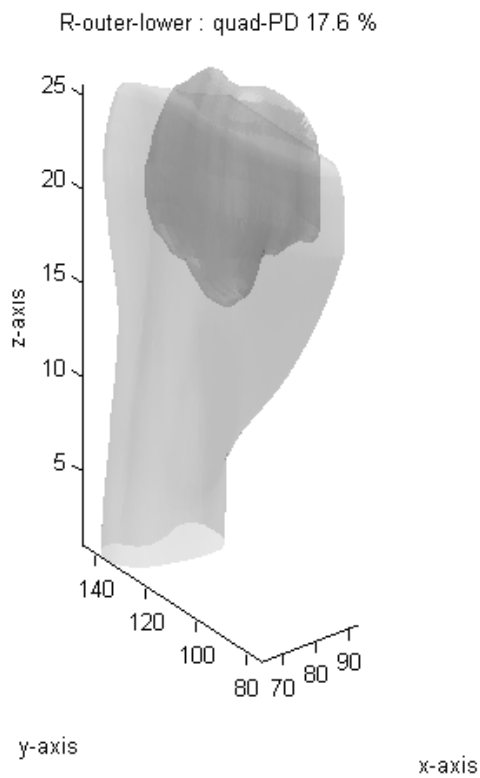


**Figure 31 Right breast outer lower quadrant**

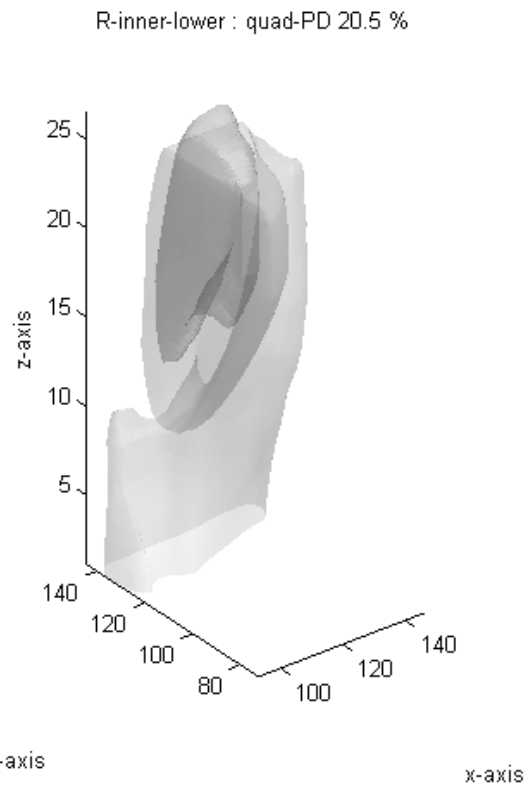


**Figure 32 Right breast inner lower quadrant**

## Chapter 5

### Summary and conclusions

In this thesis we studied several datasets obtained from breast MRI exams. The purpose was to evaluate the breast density factor, important when evaluating the development of breast cancer. The breast density factor is the ratio between the volume of fibroglandular tissue to the total volume of the breasts, and it always has to be considered by the radiologists for detection and diagnosis of breast cancer.

We first presented an analysis method to calculate this breast density factor, which is based on image segmentation algorithms. The images being segmented come from breast magnetic resonance imaging - breast MRI - which provides better results than conventional x-ray mammograms.

The breast MRI template-based segmentation method was first proposed by Muqing Lin in 2010. We discussed the method and applied it to more than 280 cases, providing the successful results and comparing them with their manually corrected version.



The method is not perfect, the main problem is that it results in undersegmentation on the last few slices. Therefore the manual correction was used to improve the results. Also, in cases where the shapes of the chest region have high variability the method will not provide optimum results.

Future work should develop a calculation on the variance between slices to be able to solve the issue, as well as be able to count with multiples templates instead of only one per case.

In this thesis we also analyzed the 3D model reconstruction of the data, based on the 2D slices of thickness between 1 and 3 mm. The method to obtain the 3D representation of the breasts as well as a video of the 3D data was demonstrated.

The 3D reconstruction tool performs a breast alignment correction, followed by the 3D reconstruction and a video generation where we can observe the 3D model from different angles and with different rotation and speed.

This 3D visualization is very helpful for radiologists, specially when comparing two MRI studies belonging to the same patients but acquired in different years, for example before and after therapy.

Finally we present a tool to divide the breast by its four quadrants. The idea behind this study is to be able to focus on the data from a specific quadrant, since the cancer risk has been demonstrated to be different depending on the area of the breast and therefore it is an interesting option for the radiologists to be able to observe a 3D representation of the desired breast quadrant.

The 3D model reconstruction, video generation and the quadrants segmentation are performed in MATLAB. Especially the video generation is a process that takes a lot of time – about 20 minutes for the video-, due to the high amount of data and slow processor. Integrating other languages and programming environments could improve the issue of slow processing.



## References

### Chapter 1

[1.1] Macmillan Cancer Support website *www.macmillan.org.uk*

[1.2] Carol DeSantis, Leah Bryan et al. *Breast cancer statistics*

[1.3] Valerie A. McCormack, *Breast density and parenchymal patterns as markers of breast cancer risk: A meta-analysis*

[1.4] Yaffe, Byng, Jong et al. *Breast cancer risk and measured mammographic density*

[1.5] Vachon, Scott, Maloney, Ghosh, Brandt et al. *Longitudinal trends in mammographic percent density and breast cancer risk.*

[1.6] Norman F. Boyd, G.S.D., Jennifer Stone, Anoma Gunasekara, Dallas R.English, Margaret R.E, Graham G. Giles, David Tritchler, Anna Chiarelli, Matin J. Yaffe, John L. Hopper, *Heritability of mammographic density, a risk factor for breast cancer.*

[1.7] Prionas, Ray, Huang, Beckett, Monsky, Boone et al. *Contrast-enhanced Dedicated Breast CT: Initial clinical experience*

## Chapter 2

[2.1] National Cancer Institute website, *www.cancer.gov*

[2.2] General Electric Healthcare website, *www.gehealthcare.com*

[2.3] Advanced Image Enhancement website, *www.aie-inc.net*

[2.4] Muqing Lin, *Development of segmentation and registration methods for analysis of Magnetic Resonance Images in clinical applications*

[2.5] Yifan Li, *Breast density analysis – Quantitative methods and 3D model reconstruction*

[2.6] Norman F. Boyd, G.S.D., Jennifer Stone, Anoma Gunasekara, Dallas R.English, Margaret R.E, Graham G. Giles, David Tritchler, Anna Chiarelli, Matin J. Yaffe, John L. Hopper, *Heritability of mammographic density, a risk factor for breast cancer.*

[2.7] Valerie A. McCormack, *Breast density and parenchymal patterns as markers of breast cancer risk: A meta-analysis*

[2.8] Yaffe, Byng, Jong et al. *Breast cancer risk and measured mammographic density*

[2.9] Vachon, Scott, Maloney, Ghosh, Brandt et al. *Longitudinal trends in mammographic percent density and breast cancer risk*

[2.10] Whitman GJ, Sheppard DG, Phelps MJ, *Breast cancer staging*

[2.11] Warner, *The role of magnetic resonance imaging in screening women at high risk of breast cancer*

[2.12] DeMartini and Lehman, *A review of current evidence-based clinical applications for breast magnetic resonance imaging*

[2.13] El Khouli, Jacobs and Bluemke, *Magnetic resonance imaging of the breast*

[2.14] Lee NA, Rusinek H, Weinreb J, Chandra R, Toth H, Singer C and Newstead G, *Fatty and fibroglandular tissue volumes in the breasts of women 20-83 years old: comparison of X-ray mammography and computer-assisted MR imaging*

[2.15] Khazen M, Warren RM, Boggis CR, Bryant EC, Reed S, Warsi I, Pointon LJ, Kwan-Lim GE, Thompson D, Eeles R, Easton D, Evans DG and Leach MO, *A pilot study of compositional analysis of the breast and estimation of breast mammographic density using three-dimensional T1-weighted magnetic resonance imaging*

[2.16] Wang, Ding and Wang, *Multistage processing procedure for 4D breast MRI segmentation*

[2.17] Lu W, Yao J, Lu C, Prindiville S and Chow C, *DCE-MRI Segmentation and motion correction based on active contour model*

[2.18] Nie K, Chen JH, Chan S, Chau MK, Yu HJ, Bahri S, Tseng T, Nalcioglu O and Su MY, *Development of a quantitative method for analysis of breast density based on three-dimensional breast MRI*

[2.19] Gallego C and Martel AL, *Automatic model-based 3D segmentation of the breast in MRI*

#### Chapter 4

[4.1] Nafiza Saidin, Harsa AmyliaMat Sakim, Umi Kalthum Ngah and Ibrahim Lutfi Shuaib, *Segmentation of breast regions in mammogram based on density: A Review*

[4.2] Kamakura, Akazawa, Nomura, Sugimachi, Nose, *Poor prognosis of lower quadrant breast carcinoma*

[4.3] Snehal M. Pinto Pereira, Valerie A. McCormack, John H. Hipwell, Carol Record, Louise S. Wilkinson, Sue M. Moss, David J. Hawkes, and Isabel Dos-Santos-Silva, *Localized fibroglandular tissue as a predictor of future tumor location within the breast*

[4.4] Snehal M Pinto Pereira, Valerie A McCormack, Sue M Moss and Isabel Dos-Santos-Silva, *The spatial distribution of radiodense breast tissue: a longitudinal study*

[4.5] Stylianos D. Tzikopoulou<sup>a</sup>, Michael E. Mavroforakis<sup>b</sup>, Harris V. Georgiou<sup>a</sup>, Nikos Dimitropoulos<sup>c</sup>, Sergios Theodoridis, *A fully automated scheme for mammographic segmentation and classification based on breast density and asymmetry*

[4.6] R. J. Ferrari, R. M. Rangayyan, J. E. L. Desautels, and A. F. Frère, *Analysis of asymmetry in mammograms via directional filtering with Gabor wavelets*

[4.7] Xingwei Wang, Dror Lederman, Jun Tan ,Xiao Hui Wang, Bin Zheng, *Computerized prediction of risk for developing breast cancer based on bilateral mammographic breast tissue asymmetry*